

# Computing the Abel map

Bernard Deconinck                      Matthew S. Patterson  
bernard@amath.washington.edu      mpatters@amath.washington.edu  
Department of Applied Mathematics  
University of Washington  
Seattle, WA 98195-2420

March 15, 2008

## Abstract

We present the next step in an ongoing research program to allow for the black-box computation of the so-called finite-genus solutions of integrable differential equations. This next step consists of the black-box computation of the Abel map from a Riemann surface to its Jacobian. Using a plane algebraic curve representation of the Riemann surface, we provide an algorithm for the numerical computation of this Abel map. Since our plane algebraic curves are of arbitrary degree and may have arbitrary singularities, the Abel map of *any* connected compact Riemann surface may be obtained in this way. This generality is necessary in order for these algorithms to be relevant for the computation of the finite-genus solutions of any integrable equation.

## 1 Introduction

This paper presents the next step in an ongoing research program to make effective the calculus on Riemann surfaces represented by plane algebraic curves. Here “effective” means that algorithms are devised and implemented in the form of black-box programs so that different relevant quantities associated with Riemann surfaces may be computed symbolically or numerically in an efficient way. Our main goal is the computation of the so-called finite-genus solutions of integrable differential (or difference) equations. Among the most famous of such systems are the Korteweg-deVries (KdV) equation and the Nonlinear Schrödinger (NLS) equation. These equations have been widely used in the last forty years for the description of various physical phenomena, ranging from water waves, nonlinear optics and plasma physics to biological applications and cellular automata [2, 1, 18]. However, in addition to the computation of solutions to these integrable equations, in the process of our work we have found that interesting unrelated problems are brought into reach. Such an example is presented here in Section 5.1.

Especially the soliton solutions of the integrable equations have found a well-deserved niche in both theory and experiment. This popularity has not been shared with their periodic and quasiperiodic counterparts. We believe that one reason for this is the inherent connection of these solutions with the theory of Riemann surfaces and theta functions. For instance, for the Kadomtsev-Petviashvili (KP) equation, the finite-genus solutions  $u(x, y, t)$  are given by

$$u = c + 2\partial_x^2 \ln \theta(\mathbf{U}x + \mathbf{V}y + \mathbf{W}t + \mathbf{A}(P^\infty, D) - \mathbf{K}|\mathbf{B}). \quad (1)$$

Here  $c$  is a constant,  $\mathbf{U}$ ,  $\mathbf{V}$  and  $\mathbf{W}$  are constant vectors;  $\theta(\mathbf{z}|\mathbf{B})$  denotes the Riemann theta function, parameterized by the Riemann matrix  $\mathbf{B}$  of an underlying Riemann surface  $\Gamma$ . Lastly,  $D$  is a divisor

of places on  $\Gamma$ ,  $\mathbf{A}(P^\infty, D)$  is its Abel map with initial place  $P^\infty$ , and  $\mathbf{K}$  is the vector of Riemann constants. More detail on all of this is found in [3], for instance. The computation of the Riemann matrix was the main topic of [13], while algorithms to compute the theta function are found in [10]. The computation of the Abel map is discussed in the present paper. Formula (1) shows that the Abel map partially determines the phase shift of finite-genus KP solutions. A similar statement is true for the finite-genus solutions of other integrable equations. A follow-up paper will present algorithms for the computation of the Riemann constant vector [11].

The reason for using the solutions of the KP equation as an example is that, in contrast to those of the KdV or NLS equation, they require the consideration of *all* compact, connected Riemann surfaces. It is an important aspect of our work that we consider arbitrary compact, connected Riemann surfaces, represented by plane algebraic curves of arbitrary degree with arbitrary singularities. Needless to say, this generality is the source of many of the difficulties we encounter.

A second remark is in order. Other approaches for the effective calculation with Riemann surfaces exist. For instance, the group at TU-Berlin is also interested in solutions of integrable systems, and they use a Schottky uniformization approach [6, 5]. This approach is equally general and has some advantages over ours. The main advantage is that their algorithms are all geometric in nature, allowing for fast implementations using floating-point numbers. In contrast, although many of our algorithms are geometric (and use floating-point numbers), they may also have to rely (in the case of singular plane curves) on algebraic structure, for which exact arithmetic is required. An advantage of our approach is that it allows us to consider the finite-gap solutions as solutions of suitable initial-value problems. This is discussed for the KP equation in [12], and for one-dimensional equations in Section 4.6 of [3]. Such an approach is beneficial for the matching of the finite-genus solutions with experimental data.

The style of this paper is similar to that of [13] and [10], where notation and definitions are kept to a minimum. This is meant to aid the interested scientist or engineer who we have in mind as potential end-users of our algorithms and black-box programs. In the same spirit of accessibility, the necessary ingredients from the theory of Riemann surfaces are described in some detail in the next section.

## 2 Problem formulation

### 2.1 Riemann surfaces from plane algebraic curves

A Riemann surface is a one-dimensional complex-analytic manifold [16]. The only topological invariant of a connected Riemann surface is its number of handles, or *genus*. A compact, connected surface  $\Gamma$  can be obtained from an irreducible plane algebraic curve  $C$  through a number of equivalent processes [25, 19]. In the algorithms we present here a Riemann surface is a branched algebraic  $y$ -cover of the complex  $x$ -sphere. We give a very brief introduction to the needed theory of Riemann surfaces from this perspective. More details can be found in the standard references [16, 25, 19, 20].

Consider an irreducible polynomial in  $x$  and  $y$

$$F(x, y) = f_0(x)y^n + f_1(x)y^{n-1} + \dots + f_n(x), \quad (2)$$

where  $x, y \in \mathbb{C}$  and the  $f_i(x)$  are polynomials in  $x$  with complex coefficients. The plane algebraic curve  $C$  is the locus of pairs  $(x, y)$  that satisfy  $F(x, y) = 0$ . We treat  $x$  as an independent variable, and by using different terms we intentionally distinguish between  $x$ -values and the  $(x, y)$ -pairs over the  $x$ -sphere.

- *Point* refers to a value of the independent variable  $x \in \mathbb{P}^1 = \mathbb{C} \cup \{\infty\}$ .

- *Place* refers to a location on the Riemann surface  $\Gamma$ . Almost all places are specified by a pair  $(x_0, y_0)$ . However, for some places it is necessary to go beyond this by specifying a pair of expansions for  $x$  and  $y$ , both in a local coordinate  $t$ . These expansions over a point  $x \in \mathbb{P}^1$  solve  $F(x, y) = 0$ , for the moment formally. Places are written as capital Roman letters, usually  $P$  or  $Q$ .

## 2.2 Points and places

A point  $\alpha \in \mathbb{C}$  is called a *regular point* if the equation

$$F(\alpha, y) = f_0(\alpha)y^n + f_1(\alpha)y^{n-1} + \dots + f_n(\alpha) = 0 \quad (3)$$

has  $n$  distinct finite roots  $y(\alpha) = \{\beta \in \mathbb{C} : F(\alpha, \beta) = 0\}$ . A point  $\alpha \in \mathbb{C}$  is a *discriminant point* if it is not regular [19], which is to say, if there are less than  $n$  distinct  $y$ -roots of (3). These are exactly the points where  $F = 0 = F_y$  where  $F_y$  is the partial derivative of  $F$  with respect to  $y$ . As  $F_y$  is also a polynomial in  $x, y$ , there are only a finite number of discriminant points [19].

The  $y$ -roots of (2) at  $x = \infty$  are defined as the roots of

$$G(X, y) = X^{\deg(F, x)} F(1/X, y) = 0,$$

where  $\deg(F, x)$  is the degree of  $F$  in  $x$  [4]. The point at  $x = \infty$  is a regular point if  $G$  has  $n$  distinct  $y$ -roots at  $X = 0$ , and a discriminant point otherwise.

Near a regular point  $\alpha \in \mathbb{P}^1$  the  $y$ -roots of (2) are given by  $n$  power series in  $x - \alpha$ . In Example 1 we calculate such a series. Near a discriminant point, representing the  $y$ -roots may require a fractional power series, known as a Puiseux series. The need for fractional powers is evident in Example 2. In Newton's Theorem we will introduce a local coordinate to remove the need for fractional power series.

**Example 1.** *The algebraic curve  $F(x, y) = y^2 - (x^3 - 1) = 0$  gives rise to a genus one Riemann surface. To find the  $y$ -roots near  $x = 0$  we solve for  $y = (-1 + x^3)^{1/2}$ , then expand formally in  $x$  to get two power series:*

$$y = \pm i \left( 1 - \frac{x^3}{2} + \frac{x^6}{8} \dots \right).$$

*To unambiguously specify the two places above  $x = 0$ , it suffices to take only the first term in each  $y$ -expansion. That is, the places are correctly specified by the pairs  $(0, i)$  and  $(0, -i)$ .*

**Example 2.** *The only discriminant points of  $y^2 - (x^3 - 1) = 0$  occur at the third roots of unity  $\alpha_j = e^{2\pi ij/3}$ ,  $j = 0, 1, 2$ , where the single root is  $y = 0$ . To find  $y = y(x)$  near  $\alpha_j$  let  $x = \alpha_j + t$ . For convenience we choose to work near  $x = \alpha_0 = 1$ , then the  $y$ -roots are given by*

$$y = \pm ((1+t)^3 - 1)^{\frac{1}{2}} = \pm (3t + 3t^2 + t^3)^{\frac{1}{2}} = \pm \sqrt{3} t^{\frac{1}{2}} \left( 1 + t + \frac{t^2}{3} \right)^{\frac{1}{2}}$$

*We expand in  $t$ , rearrange and back substitute to get a fractional power series in  $x - 1$*

$$y(x) = \pm \sqrt{3} \left( (x-1)^{\frac{1}{2}} + \frac{(x-1)^{\frac{3}{2}}}{2} + \frac{(x-1)^{\frac{5}{2}}}{24} + \dots \right). \quad (4)$$

*The presence of fractional powers in (4) defines  $\alpha_0$  to be a branch point. A similar conclusion is easily reached for  $\alpha_1, \alpha_2$ .*

The following statement of Newton's Theorem is an abridged version of that in [4], and establishes the existence of the series found in these examples.

**Newton's Theorem.** *In a neighborhood of  $\alpha$ , the  $n$   $y$ -roots of  $F(x, y) = 0$  are determined by a finite number of pairs of expansions of the form*

$$P_j = \begin{cases} x &= \alpha + t^{r_j} \\ y &= \beta_j t^{s_j} + \beta'_j t^{s'_j} + \dots \end{cases}, \quad (5)$$

where  $\alpha, r_j, \beta_j, \beta'_j, s_j$  and  $s'_j$  are as described below.

- **Finite places:** *A place is called finite if both the  $x$ - and  $y$ -components are finite for  $t = 0$ . For each finite place we have the following properties.*
  - *The branching number  $r_j$  counts the number of  $y$ -roots that coalesce at the place  $P_j$ . If  $r_j > 1$  for one of the  $P_j$ , then  $\alpha$  is a branch point.*
  - *For  $|t| > 0$ , a place  $P_j$  represents  $r_j$  distinct  $y$ -values. Further,  $\sum_j r_j = n$ .*
  - *The coefficients  $\beta_j, \beta'_j, \dots \in \mathbb{C}$  are all non-zero.*
  - *The exponents  $r_j, s_j, s'_j, \dots \in \mathbb{Z}$  are positive (or zero) and have no overall common factor.*
- **Infinite places:** *Infinite places are those for which one or both components are infinite for  $t = 0$ . This occurs only when  $\alpha = \infty$  or  $f_0(\alpha) = 0$ , where  $f_0$  is the leading polynomial coefficient of (2). Infinite places have the same properties as finite places except:*
  - *the  $y$ -components may have a finite number of negative exponents  $s, s'$ , and*
  - *for places over  $x = \infty$ , the  $x$ -components have  $x = 1/t^r$  replacing  $x = \alpha + t^r$ .*

Two places as above are equivalent if the substitution  $t \rightarrow \xi t$ , with  $\xi$  an  $r_j$ -th root of unity, identifies them. Away from  $t = 0$ , two equivalent places determine the same set of  $y$ -roots of  $F(x, y) = 0$ . Away from  $t = 0$ , non-equivalent places determine disjoint sets of  $y$ -roots.

In general, the  $x$ -component of a place can be written as  $x = \alpha + \alpha' t^r$  (or  $x = \alpha'/t^r$ ), but for convenience we choose  $\alpha' = 1$ . Any choice  $\alpha'$  is possible, but the  $\beta, \beta', \dots$  reflect this choice.

The  $y$ -component in Newton's Theorem converges at least over the punctured disc  $\mathcal{R}$ , where

$$\mathcal{R} = \{x : |x - \alpha| < |\alpha - \lambda|, x \neq \alpha\}. \quad (6)$$

and  $\lambda \neq \alpha$  is the discriminant point closest to  $\alpha$ . This restriction on the radius of  $\mathcal{R}$  arises as  $\lambda$  is the nearest point (distinct from  $\alpha$ ) where it is possible the derivative  $dy/dt = -F_x/F_y$  is not defined. Convergence of places over regular points is established in [4]. In this case the roots of  $F = 0$  are represented as  $n$  convergent series in  $t = x - \alpha$  on the disc  $\mathcal{R} \cup \{\alpha\}$  (unpunctured).

If  $\alpha$  is a discriminant point, then convergence of the  $y$ -component is questionable at  $x = \alpha$ . For now we consider  $\alpha$  to be a non-branch discriminant point (the convergence of the  $y$ -series over branch points is discussed in Section 2.3). Suppose  $P$  is given by

$$\begin{cases} x &= \alpha + t \quad (\text{or } 1/t \text{ over } \infty) \\ y &= \beta t^s + \beta' t^{s'} + \dots \end{cases}, \quad (7)$$

with  $\alpha$  (or  $\infty$ ) a non-branch discriminant point. The expansion

$$y = \beta(x - \alpha)^s + \beta'(x - \alpha)^{s'} + \dots \quad (8)$$

is unique and convergent at least on  $\mathcal{R}$ . Convergence of (7) over  $x = \alpha$ , that is for  $t = 0$ , depends on whether the  $x$ - and  $y$ -components of  $P$  are finite there.

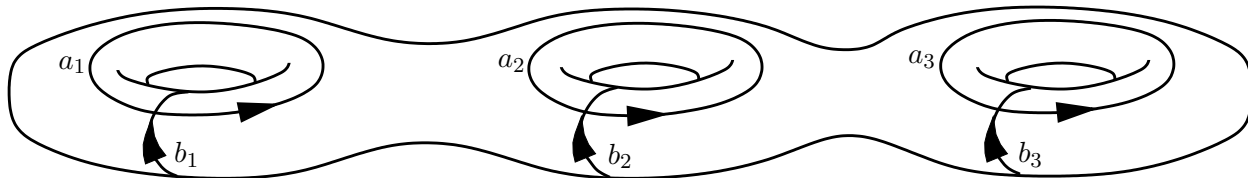


Figure 1: An idealization of a genus three Riemann surface. The paths indicated in this figure are the  $a$ - and  $b$ -cycles that form a basis of cycles on  $\Gamma$  (see Section 2.4). The  $a$ -cycles go around the holes, and the  $b$ -cycles encircle the handles. The  $a$ - and  $b$ -cycles shown indeed have the intersection indices required by Equations (12).

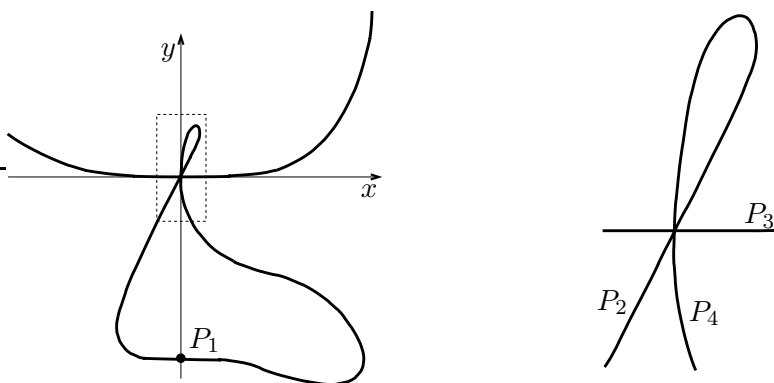


Figure 2: A plot of the real part of  $F = -y^5 + (2x-1)y^4 - (3x-x^2)y^3 - (x-3x^2)y^2 + (x^3-2x^2)y + x^6$ . The figure on the right is an enlarged view of the part of the graph on the left enclosed by the box.

- **Finite places** ( $x, y \in \mathbb{C}$ ): For finite places no  $s, s', \dots$  is negative, and (8) is the unique power series expansion valid on  $\mathcal{R} \cup \{\alpha\}$ .
- **Infinite places (i)** ( $x \in \mathbb{C}, y = \infty$ ): Such places occur over points  $x = \alpha$  for which the leading polynomial coefficient  $f_0(\alpha) = 0$ , where  $f_0$  is as in (2). In this case a finite number of the  $s, s', \dots$  will be negative and (8) is the unique Laurent series expansion in  $x - \alpha$ , convergent on  $\mathcal{R}$ .
- **Infinite places (ii)** ( $x, y = \infty$ ): If  $x = \infty$  is not a branch point, then each place over  $\infty$  is of the form

$$\begin{cases} x = 1/t \\ y = \beta t^s + \beta' t^{s'} + \dots \end{cases},$$

where a finite number of  $s, s', \dots$  are negative. That is,  $y(t)$  is a unique Laurent series expansion in  $t$ , where  $t = 1/x$  is an analytic function for finite  $x$ . Thus  $y(t)$  is convergent on

$$\mathcal{R}_\infty = \{x : |x| > \lambda_{\max}, x \neq \infty\}$$

where  $\lambda_{\max}$  is the finite discriminant point with largest absolute value.

Given an irreducible polynomial  $F(x, y)$ , the union of all places over all  $x \in \mathbb{P}^1$  is a finite genus compact, connected Riemann surface [19]. Figure 1 shows an idealization of a genus three Riemann surface. The actual surface defined by an algebraic curve  $C$  is a two-real-dimensional manifold embedded in a four-dimensional space. The example that follows demonstrates the use of Puiseux expansions to determine the local structure of a plane algebraic curve.

**Example 3.** Over the point  $x = 0$ , the five  $y$ -roots of the polynomial

$$F = -y^5 + (2x - 1)y^4 + (3x - x^2)y^3 + (x - 3x^2)y^2 + (x^3 - 2x^2)y + x^6$$

are represented by the four places

$$P_1 = \begin{cases} x &= t \\ y &= -1 - t^3 + \dots \end{cases}, \quad P_2 = \begin{cases} x &= t \\ y &= 2t + t^2 + \dots \end{cases}, \\ P_3 = \begin{cases} x &= t \\ y &= t^4/2 + t^5/4 + \dots \end{cases}, \quad P_4 = \begin{cases} x &= t^2 \\ y &= t - t^3/2 + \dots \end{cases}.$$

Note that, as opposed to Example 1, here the first terms in the  $y$ -expansions do not suffice to unambiguously specify the places, but only distinguishes  $P_1$  from the remaining three places. A graph of the real part of  $F$  near  $(x, y) = (0, 0)$  is seen in Fig. 2. We determine which part of the graph correspond to which place in the example by calculating  $dy/dx$  for each  $P_j$ . Place  $P_1$  is easily identified in the figure as it is the only place where  $y \neq 0$  for  $x = 0$ . For  $P_2$  and  $P_3$ , make the simple substitution  $t = x$  in the series for  $y$ . At place  $P_2$ ,  $y$  and its derivative are

$$y = 2x + x^2 + \dots, \quad \frac{dy}{dx} = 2 + 2x + \dots.$$

The correct match for place  $P_2$  is clear as  $dy/dx|_{x=0} = 2$  and there is only one component of the graph which has positive finite slope near  $x = 0$  so the match is clear. For place  $P_3$

$$y = x^4/2 + x^5/4 + \dots, \quad \frac{dy}{dx} = 2x^3 + 5x^4/4 + \dots.$$

As here  $dy/dx|_{x=0} = 0$ , this is also easy to match. At place  $P_4$ , we parametrically differentiate

$$\frac{dy}{dx} = \frac{\partial y / \partial t}{\partial x / \partial t} = \frac{1 - 3t^2/2 + \dots}{2t} = \frac{1}{2t} - \frac{3}{4}t + \dots.$$

Thus place  $P_4$  matches the component of the graph for which  $dy/dx$  is undefined at  $t = 0$ . Note that  $x = 0$  is a branch point since  $x$  is not linear in  $t$  for  $P_4$ .

## 2.3 Branches

Over a regular point  $\alpha$  there are  $n$  distinct places and the terms “place” and “branch” are equivalent. Over a branch point  $\alpha$  there are less than  $n$  places, and thus there are some number of places over  $\alpha$  for which the branching number  $r > 1$ . Let

$$P = \begin{cases} x &= \alpha + t^r \\ y &= \beta t^s + \beta' t^{s'} + \dots \end{cases}, \quad (9)$$

where  $|r| > 1$ , be such a place. From the place  $P$ , form the  $r$  branches

$$\tilde{P}_j = \begin{cases} x &= \alpha + (e^{2\pi i j / r} t)^r = \alpha + t^r \\ y_j &= \beta (e^{2\pi i j / r} t)^s + \beta' (e^{2\pi i j / r} t)^{s'} + \dots \end{cases} \quad \arg(t) \in [0, 2\pi / r), \quad (10)$$

where “branch” signifies that the argument of  $t$  is restricted as indicated. As  $r, s, s', \dots$  are coprime, the  $y_j$  in (10) are all distinct. Further the  $y$ -series in (9) is related to the  $j$ -th series in (10) by  $y_j(e^{-2\pi i j / r} t) = y(t)$ . The index  $j$  may be chosen such that  $\exp(-2\pi i(j)/r)t$  has argument restricted

to  $[0, 2\pi/r)$ . Thus the  $r$  distinct roots represented by place  $P$  are also represented by  $\tilde{P}_1, \dots, \tilde{P}_r$ , with  $\arg(t)$  restricted.

Suppose that  $\lambda \neq \alpha$  is the nearest discriminant point to  $\alpha$ , and let  $\mathcal{R}$  be given as in 6. The points  $x \in \mathcal{R}$  are all represented exactly once by  $x = \alpha + t^r$  if the argument of  $t$  is restricted as in (10). Restricting  $t$  this way makes  $t(x)$  the single valued function  $t = \sqrt[r]{x - \alpha}$ , where here and subsequently we denote by  $\sqrt[r]{\xi}$  the  $r$ -th root of  $\xi$  with argument on  $[0, 2\pi/r)$ . Thus defined,  $t(x)$  is analytic on  $\mathcal{R}$ . Each of the  $y$ -series is analytic in  $t$ , as noted in Section 2.2, and so the  $n$  roots of (3) are represented as  $n$  series which are convergent up to the nearest distinct discriminant point.

## 2.4 Paths and cycles

A *path*  $\gamma$  on  $\Gamma$  is a parameterized curve  $\gamma : z \rightarrow (x(z), y(z))$  such that  $F(x(z), y(z)) = 0$  and for convenience  $z \in [0, 1]$ . A path is called closed if  $\gamma(0) = \gamma(1)$ . A closed path that bounds a part of  $\Gamma$  can be contracted to a point (*i.e.* it is homologous to zero), and is therefore trivial for the purposes of integrating analytic functions. A *cycle* on  $\Gamma$  is a closed path that is not homologous to zero. On a Riemann surface of genus  $g$  there exists a basis for its homology given by

$$\mathcal{H} = \{a_1, \dots, a_g, b_1, \dots, b_g\}, \quad (11)$$

- such that no cycle in  $\mathcal{H}$  is continuously deformable into any other, and
- all possible cycles on  $\Gamma$  are sums<sup>1</sup> of cycles in  $\mathcal{H}$ .
- Further, letting  $c_j \circ c_k$  denote the number of oriented intersections<sup>2</sup> of the cycles  $c_j$  and  $c_k$  and  $\delta_{jk}$  denote the Kronecker delta [13], we have

$$a_j \circ a_k = 0, \quad b_j \circ b_k = 0, \quad a_j \circ b_k = \delta_{jk}, \quad (12)$$

We may think of the  $a$  cycles as encircling the holes, and the  $b$  cycles as going around the handles of  $\Gamma$ , as shown in Figure 1. A representation of the homology of a Riemann surface associated with a plane algebraic curve can be explicitly calculated by the Maple command `algcurves[homology]` [13].

## 2.5 Differentials

A *holomorphic differential* is an integrand, or one-form,

$$\tilde{\omega}_j = \frac{p_j(x, y)}{F_y} dx, \quad (13)$$

that has no poles on  $\Gamma$  and transforms via the chain rule. The polynomials  $p_j$  in (13) have the form

$$p_j(x, y) = \sum_{k+m \leq d} c_{jkm} x^k y^m,$$

where  $d = \deg(F, y) - 3$ . Imposing the regularity of  $\tilde{\omega}_j$  at the discriminant points of  $F$  constrains the polynomials  $p_j(x, y)$  such that on a genus  $g$  Riemann surface it is possible to construct exactly

---

<sup>1</sup>By the *sum* of two cycles,  $c_j$  and  $c_k$  is meant to first traverse cycle  $c_j$  and then cycle  $c_k$ . The cycle  $c_j$  traced backward is  $-c_j$ .

<sup>2</sup>If the cycles  $c_j$  and  $c_k$  do not intersect, then  $c_j \circ c_k = 0$ . If  $c_j$  and  $c_k$  intersect once, then  $c_j \circ c_k = \pm 1$ , where the sign of the intersection index is the orientation of the basis  $(\mathbf{t}_j, \mathbf{t}_k)$ . Here  $\mathbf{t}_j, \mathbf{t}_k$  are the unit tangent vectors of the cycles  $c_j$  and  $c_k$  respectively at the point of intersection. For cycles with multiple intersections,  $c_j \circ c_k$  is computed as the sum over all intersections, each one treated as a single intersection.

$g$  linearly independent, holomorphic differentials in this form [13, 19]. Further, by taking linear combinations of the  $\tilde{\omega}_i$ , one may choose a  $g$ -dimensional basis of normalized holomorphic differentials

$$\{\omega_1, \dots, \omega_g\}, \quad \oint_{a_k} \omega_j = \delta_{jk}, \quad (14)$$

where the  $a_j$  are from (12). A basis of the holomorphic differentials on a Riemann surface arising from an algebraic curve is computed by the Maple command `algcures[differentials]` [13].

## 2.6 Riemann matrices and the Jacobian

Integration of normalized differentials around the remaining  $b$  cycles defines the *Riemann matrix*

$$\mathbf{B} = (B_{j,k})_{j,k=1}^g, \quad B_{j,k} = \oint_{b_k} \omega_j. \quad (15)$$

A Riemann matrix is invertible, symmetric, and has positive definite imaginary part [13, 14]. The  $(g \times 2g)$  matrix  $[\mathbf{1} \ \mathbf{B}]$ , where  $\mathbf{1}$  is the  $(g \times g)$  identity matrix, contains all the information about integrating holomorphic differentials around closed paths and is called the *normalized period matrix* of  $\Gamma$ . The columns of the period matrix are linearly independent and describe a lattice

$$\Lambda = \{\mathbf{V} = \mathbf{1}\mathbf{M} + \mathbf{B}\mathbf{N}; \ \mathbf{M}, \mathbf{N} \in \mathbb{Z}^g\}. \quad (16)$$

The quotient space

$$J(\Gamma) = \mathbb{C}^g / \Lambda \quad (17)$$

is topologically a  $2g$ -dimensional torus called the *Jacobian* of the Riemann surface<sup>3</sup>  $\Gamma$  [14, 19]. The notation  $\mathbf{V} \equiv \mathbf{W}$  is consistently used to indicate that  $\mathbf{V} - \mathbf{W} \in \Lambda$ . A Riemann matrix of an arbitrary algebraic curve given by a polynomial  $F$  is explicitly computed using the Maple command `algcures[periodmatrix](F, x, y, 'Riemann')`.

## 2.7 Divisors

A *divisor* on a Riemann surface  $\Gamma$  is a set of places with multiplicities. A divisor  $\mathcal{D}$  is written as

$$\mathcal{D} = \sum_j p_j P_j,$$

where  $p_j P_j$  denotes that the place  $P_j$  has multiplicity  $p_j$ . Divisors may be negated and added:

$$\begin{aligned} -\mathcal{D} &= \sum_j (-p_j) P_j; \\ \mathcal{D}' &= \sum_j p'_j P'_j, \quad (\mathcal{D} + \mathcal{D}') = \sum_j p_j P_j + \sum_j p'_j P'_j. \end{aligned}$$

The *degree* of a divisor is the sum of the multiplicities, denoted  $\deg \mathcal{D} = \sum_j p_j$ .

A meromorphic function  $u$  on  $\Gamma$  that has zeros  $P_1, \dots, P_m$  with multiplicities  $p_1, \dots, p_m$  and poles  $Q_1, \dots, Q_n$  with multiplicities  $q_1, \dots, q_n$  defines a divisor

$$(u) = \sum_j p_j P_j - \sum_j q_j Q_j.$$

---

<sup>3</sup>Choosing a different basis of cycles  $\mathcal{H}'$  results in a different Riemann matrix  $\mathbf{B}'$ , however  $\mathbf{B}$  and  $\mathbf{B}'$  are related by a symplectic transformation, and the Jacobians induced by both are identical [14].

Similarly, the divisor  $(\omega)$  of a differential  $\omega$  that has zeros  $P_1, \dots, P_m$  with multiplicities  $p_1, \dots, p_m$  and poles  $Q_1, \dots, Q_n$  with multiplicities  $q_1, \dots, q_n$  is

$$(\omega) = \sum_{j=1}^m p_j P_j - \sum_{j=1}^n q_j Q_j.$$

Two divisors  $\mathcal{D}$  and  $\mathcal{D}'$  are *linearly equivalent* if  $\mathcal{D} - \mathcal{D}'$  is the divisor of a meromorphic function [14, 19]. If  $\omega$  and  $\omega'$  are Abelian differentials, then

$$(\omega) - (\omega') = \sum_j p_j P_j - \sum_j q_j Q_j - \left( \sum_j p'_j P'_j - \sum_j q'_j Q'_j \right) = \left( \frac{\omega}{\omega'} \right),$$

and  $\omega/\omega'$  is a meromorphic function on  $\Gamma$ . Thus the divisors of any two meromorphic differentials are linearly equivalent. They belong to the *canonical class* of divisors. The degree of any divisor in the canonical class is  $2g - 2$  [19]. Abelian differentials are distinguished by their pole structure.

- Abelian differentials of the first kind are holomorphic differentials.
- Abelian differentials of the second kind have a single pole of order greater than one.
- Abelian differentials of the third kind have two simple poles with residues  $+1$  and  $-1$ .

Any Abelian differential is a linear combination of these kinds of differentials [25]. The divisors of all Abelian differentials constitute the full class of canonical divisors [14].

## 2.8 The Abel map

The Abel map of a place  $P$  on a genus  $g$  Riemann surface is defined by

$$A = (A_1, \dots, A_g) : \quad A_j(P', P) = \int_{P'}^P \omega_j, \quad (18)$$

where  $P'$  is a fixed place on the Riemann surface, the  $\omega_j$  are normalized as in (14) and the path of integration is the same for each  $j$  [14]. Equation (18) can be written in vector form as

$$\mathbf{A} : \Gamma \rightarrow J(\Gamma) = \mathbf{A}(P', P) = \int_{P'}^P \boldsymbol{\omega}$$

where  $\boldsymbol{\omega} = (\omega_1, \dots, \omega_g)$ . The difference between any two paths  $\gamma$  and  $\eta$  is

$$\gamma - \eta = \sum_{j=1}^g m_j a_j + \sum_{j=1}^g n_j b_j$$

where  $m_i, n_i$  are integers and the  $a_i, b_i \in \mathcal{H}$ . Thus the Abel map of a place  $P$  is well defined in that its image is an element of  $J(\Gamma)$ .

The definition of the Abel map is extended to divisors  $\mathcal{D}$ , written in vector notation, as

$$\mathbf{A}(P', \mathcal{D}) = \sum_i p_i \mathbf{A}(P', P_i).$$

Abel's theorem sheds more light on what it means for divisors to be linearly equivalent. This phrasing of Abel's Theorem is from [19].

**Abel’s Theorem.**

- For any meromorphic function  $u$  on  $\Gamma$  with  $(u) = \mathcal{D}$  we have  $\mathbf{A}(P', \mathcal{D}) \equiv 0$ .
- Given a degree zero divisor  $\mathcal{D}$  such that  $\mathbf{A}(P', \mathcal{D}) \equiv 0$ , there exists a meromorphic function  $u$  such that  $(u) = \mathcal{D}$ .

The Abel map of a degree zero divisor is independent of the initial point  $P'$ . This is seen by writing  $\mathcal{D}$  as  $\mathcal{D} = \sum_{j=1}^m (P_j - Q_j)$  where points may appear multiple times. The Abel map is then

$$\mathbf{A}(P', \mathcal{D}) = \sum_{j=1}^m \left( \int_{P'}^{P_j} \omega - \int_{P'}^{Q_j} \omega \right) = \sum_{j=1}^m \int_{Q_j}^{P_j} \omega.$$

A direct consequence of Abel’s Theorem is that two divisors  $\mathcal{D}$  and  $\mathcal{D}'$  differ by the divisor of a meromorphic function if and only if (i)  $\deg \mathcal{D} = \deg \mathcal{D}'$  and (ii)  $\mathbf{A}(\mathcal{D}) \equiv \mathbf{A}(\mathcal{D}')$ . Thus linearly equivalent divisors map to the same vector on  $J(\Gamma)$  under the Abel map.

### 3 Details of the algorithm

Our input for computing  $\mathbf{A}(P', P)$  is (i) a Riemann surface  $\Gamma$ , entered as a polynomial  $F$  in two complex variables  $x, y$  and (ii) two places  $P'$  and  $P$  on  $\Gamma$ , entered as Puiseux expansion as in Newton’s theorem. Places are entered as truncated Puiseux expansions to avoid potential ambiguity at places over discriminant points, and at infinity. For places over regular points it suffices to enter an  $x, y$  pair.

To integrate along a path on  $\Gamma$  we first create a path  $\chi$  on the  $x$ -Riemann sphere  $\mathbb{P}^1$  and then lift that path to  $\Gamma$ . Correctly lifting the path introduces most of the difficulty in numerically computing the Abel map. In this section we provide the details of this process. We begin by discussing paths built to avoid all but one discriminant point. These paths and their constituents are the primary method of transportation on our surfaces. Further, these paths allow us to compute the monodromy of an algebraic curve, used to integrate from one sheet to another. Next we describe how paths are constructed to regular points, discriminant points and infinity. Thereafter we detail how paths are lifted correctly from  $\mathbb{P}^1$  to  $\Gamma$ . We conclude this section by briefly describing how the integration is carried out. Before proceeding we need to introduce some notation and a few definitions.

- In what follows  $C(\alpha, \rho)$  denotes the circle in the complex  $x$ -plane with center  $x = \alpha$  and radius  $\rho$ . By  $L(\alpha, \alpha')$  we indicate the straight line segment in the complex plane from  $\alpha$  to  $\alpha'$ .
- The “left point,”  $\alpha^\ell \in \mathbb{C}$ , is an algorithmically chosen point depending only on the polynomial  $F$ . If the set of finite discriminant points of  $F(x, y) = 0$  is  $\widehat{\lambda}$ , then  $\alpha^\ell$  is chosen such that

$$\Re(\alpha^\ell) < \Re(\lambda_j), \quad \forall \lambda_j \in \widehat{\lambda},$$

that is,  $\alpha^\ell$  is to the left (in the complex plane) of all the finite discriminant points.

- Denote by  $\mathbf{y}^\ell = (y_1^\ell, \dots, y_n^\ell)$  the *ordered* roots of  $F(\alpha^\ell, y) = 0$ , where the order is based on the absolute values and arguments of the roots. The “left place” is  $P^\ell = (\alpha^\ell, y_1^\ell)$ .
- The ordered  $n$ -tuple  $\mathbf{y}^\ell$  can be analytically continued anywhere on  $\mathbb{P}^1/\widehat{\lambda}$ . The  $n$ -tuple of complex numbers  $\mathbf{y}^\ell(\chi)$  is the result of analytically continuing each component of  $\mathbf{y}^\ell$  along the path  $\chi = x(z) \in \mathbb{P}^1/\widehat{\lambda}$ .

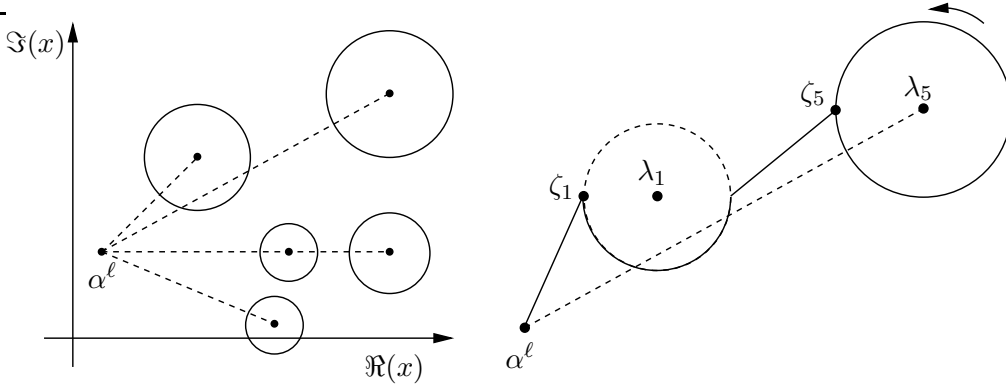


Figure 3: On the left are straight lines  $L(\alpha^\ell, \lambda_j)$  (dashed) and circles  $C_j$  (solid). On the right we isolate  $\alpha^\ell$ ,  $C_1$  and  $C_5$  in order to demonstrate how the path encircling only  $\lambda_5$  is deformed through a region to stay well away from  $\lambda_1$ . Using the terminology of Section 3.1, the solid line on the right is the path  $\chi'_5$ : the path to  $\zeta_5$  deformed once and homotopic to the line  $L(\alpha^\ell, \zeta_5)$  (not shown).

- If  $\chi$  and  $\chi'$  are two paths in  $\mathbb{P}^1/\hat{\lambda}$  with  $\chi(0) = \chi'(0)$  and  $\chi(1) = \chi'(1)$ , it is not necessary that  $\mathbf{y}^\ell(\chi) = \mathbf{y}^\ell(\chi')$ . If  $\chi$  and  $\chi'$  differ only by a circle around exactly one branch point then  $\mathbf{y}^\ell(\chi') = \sigma(\mathbf{y}^\ell(\chi))$ , where  $\sigma(\mathbf{v})$  denotes a permutation.
- To order the places over a regular point  $\alpha$  we impose the order of the  $y$ -values in  $\mathbf{y}^\ell(L(\alpha^\ell, \alpha))$ . Note that if the straight line segment  $L(\alpha^\ell, \alpha)$  happens to pass through a discriminant point  $\lambda_k$ , then the path to  $\alpha$  is adjusted to pass above  $\lambda_k$ . In this way we define the *sheets* of the Riemann surface. A place  $P = (\alpha, \mu)$  is said to lie on sheet  $j$  if

$$\left(\mathbf{y}^\ell(L(\alpha^\ell, \alpha))\right)_j = \mu.$$

Note that, as  $\mathbf{A}(P', P)$  is given by

$$\int_{P'}^P \omega = \int_{P^\ell}^P \omega - \int_{P^\ell}^{P'} \omega,$$

it suffices to develop an algorithm to compute integrals from  $P^\ell$  to any other place  $P$ .

### 3.1 Paths on the Riemann sphere

Let  $F$  be a polynomial as in (2). Further let  $\hat{\lambda} = \{\lambda_1, \dots, \lambda_m\}$  be the set of finite discriminant points of  $F(x, y) = 0$ . We now construct paths on the Riemann sphere that in Section 3.2 will be lifted to the Riemann surface  $\Gamma$  arising from  $F$ .

- **Paths avoiding discriminant points:** Around each  $\lambda_j \in \hat{\lambda}$  we compute a radius  $\rho_j$ , that is two-fifths of the distance to the next nearest discriminant point:

$$\rho_j = \frac{2}{5} \min\{|\lambda_j - \lambda_k|\}, \quad j \neq k, \quad k = 1, \dots, m.$$

Let  $C_j$  denote the circle  $C(\lambda_j, \rho_j)$ . The  $y$ -sheets are sufficiently well separated, and numerical analytic continuation works well on all paths that lie completely outside all  $C_j$ 's.

Let  $\zeta_j$  denote the point  $\lambda_j - \rho_j$ . A path  $\chi_j$  to each  $\zeta_j$  is created as follows.

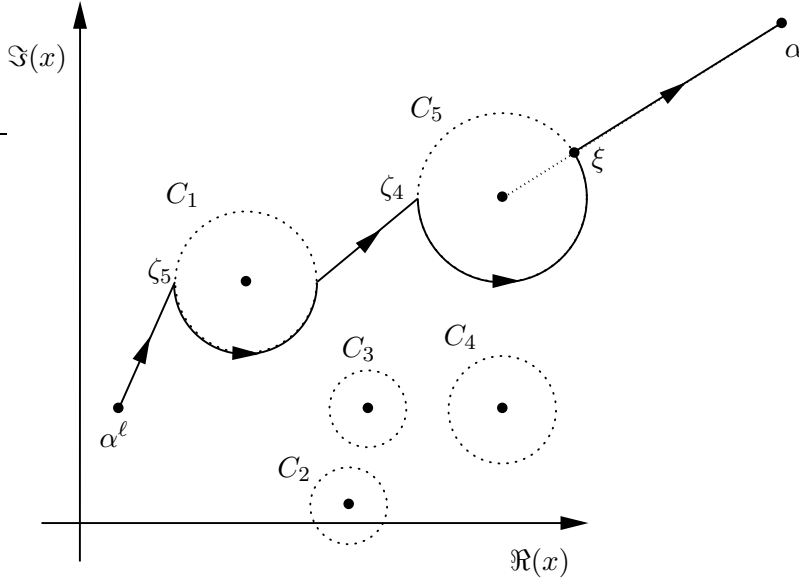


Figure 4: The solid lines and arcs indicate a path  $\chi$  in the complex  $x$ -plane to the point  $\alpha$ . These paths are lifted to the Riemann surface via numerical analytic continuation. Note that this path *not* homotopic to  $L(\alpha^\ell, \alpha)$ . It need not be. The  $n$  images of this path on  $\Gamma$  are computed, and the correct image is chosen.

1. If the line  $L(\alpha^\ell, \zeta_j)$  does not intersect any other  $C_k$  then  $\chi_j = L(\alpha^\ell, \zeta_j)$ .
2. If the line  $L(\alpha^\ell, \zeta_j)$  intersects circle  $C_k$ , then  $\chi_j$  is deformed to  $\chi'_j$ , which traverses half of  $C_k$ . Path  $\chi'_j$  includes either the top or bottom half of  $C_k$ , depending on which path is homotopic to  $L(\alpha^\ell, \zeta_j)$ . The right side of Figure 3 shows an example of this deformation.
3. If the newly deformed path  $\chi'_j$  infringes on circle  $C_m$ , then it is deformed to  $\chi''_j$ , which traverses half of  $C_m$  as in the previous step.
4. Steps 2 and 3 are iterated until a path  $\chi_j^{\dots'}$  is constructed that avoids all  $C_i$ , for  $i \neq j$ .

The path  $\Pi_j$  around discriminant point  $\lambda_j$  is then, dropping the primes,  $\chi_j$  followed by the circle  $C_j$  traversed counter-clockwise and ending with  $\chi_j$  traversed backwards. The solid line on the right of Figure 3 is such a path. The  $\Pi_j$  are used to calculate the monodromy group of  $F$  [13] and the  $\chi_j$  serve as the basic building blocks of paths to any  $\alpha \in \mathbb{P}^1$ .

- **The monodromy group:** If the point  $\lambda_j$  is a branch point, then the analytic continuation  $\mathbf{y}^\ell(\Pi_j)$  does not match up with  $\mathbf{y}^\ell$  itself. Instead  $\mathbf{y}^\ell(\Pi_j) = \sigma_j(\mathbf{y}^\ell)$ , where  $\sigma_j(\mathbf{v})$  is the permutation of the  $n$ -tuple  $\mathbf{v}$  induced by analytically continuing  $\mathbf{v}$  around branch point  $\lambda_j$ . The collection of all the permutations  $\sigma_j$  gives a representation of the monodromy group of the curve  $F$  [13]. A procedure to compute the monodromy of an arbitrary irreducible plane algebraic curve is available as the Maple command `algcurves[monodromy]`. Our implementation uses this command unaltered to compute the branch points and the permutations around those branch points.
- **Path to a finite point not near a discriminant point:** If  $\alpha$  does not lie in one of the  $C_k$ , then we construct a path  $\chi$  from  $\alpha^\ell$  to  $\alpha$  as follows. Suppose  $\lambda_j$  is the closest discriminant point to  $\alpha$ . The line  $L(\alpha, \lambda_j)$  intersects  $C_j$  at the point  $\xi$ . The path  $\chi$  is then (i) the previously discussed path  $\chi_j$  to  $\zeta_j$  followed by (ii) the arc on  $C_j$  from  $\zeta_j$  to  $\xi$ , traversed counter-clockwise,

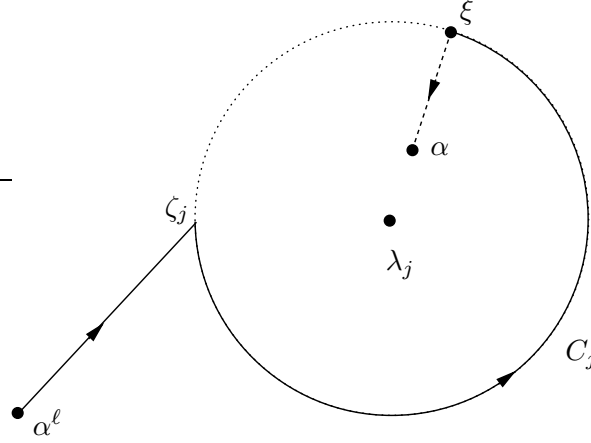


Figure 5: The solid and dashed lines together form a path from  $\alpha^\ell$  to  $\alpha$ . The solid line is lifted to the Riemann surface  $\Gamma$  by numerical analytic continuation. The dashed line is lifted by means of Puiseux expansions. The dotted line again indicates the circle around the discriminant point  $\lambda_j$  with radius  $\rho_j$ . As in Figure 4, the path shown is not, and need not be, homotopic to  $L(\alpha^\ell, \alpha)$ .

and finally (iii) the line  $L(\xi, \alpha)$ . This path avoids all  $C_k$  for  $j \neq k$  by virtue of the construction of the previously discussed paths  $\chi_j$ . Figure 4 demonstrates a path to a regular point  $\alpha$  that is closer to discriminant point  $\lambda_5$  than any other.

- **Path to a point near a discriminant point:** If the final point  $\alpha$  is inside  $C_j$ , then the path  $\chi$  is constructed as follows. Denote by  $\xi$  the point on  $C_j$  such that  $L(\lambda_j, \xi)$  contains  $\alpha$ . Then the path  $\chi$  is, as in Figure 5,

1. the path  $\chi_j$  to  $\zeta_j$ ,
2. the arc on  $C_j$  from  $\zeta_j$  to  $\xi$ , traversed counter-clockwise, and finally
3. the line segment from  $\xi$  inward towards  $\lambda_j$  to  $\alpha$ .

Note that, as far as the creation of a path is concerned, it does not matter if  $\alpha = \lambda_j$ .

- **Infinity:** If  $\alpha = \infty$ , then we pick a point  $\xi \in \mathbb{R}$  such that

$$|\xi| = \frac{5}{2} \max |\lambda|, \lambda \in \hat{\lambda}.$$

The path  $\chi$  to  $\alpha = \infty$  is then  $L(\alpha^\ell, \xi)$  followed by  $L(\xi, \infty)$ , where the line “to infinity” is traversed by the transformation  $x = 1/t$  as  $t \mapsto 0$ .

- **Navigating between sheets:** We have constructed a path  $\chi$  on the Riemann sphere from the algorithmically determined point  $\alpha^\ell$  to a generic point  $\alpha$  given by the user-specified place  $P = (x, y) = (\alpha, \mu)$ . The path  $\chi$  has  $n$  images on  $\Gamma$ . From these possible images we chose  $\gamma \in \Gamma$  such that the  $y$ -value of  $\gamma(1) = \mu$ . Let  $k$  be the index of the place  $\gamma(0)$  over  $\alpha^\ell$ . If  $k = 1$ , then the lift of  $\chi$  is exactly a path on  $\Gamma$  from the left place  $P^\ell$  to the user-specified place  $P$ . If not we make use of the monodromy group of  $F$  to create a path that will permute sheet 1 into sheet  $k$ .

From the output of the Maple command `algcures[monodromy]` we build a table  $\mathcal{M}$  that has as its entry  $\mathcal{M}_{ij}$  a list of branch points  $\lambda_1, \lambda_2, \dots$  to encircle in order to permute sheet  $m$  to sheet  $m'$  [13]. For example, if the 3,5 entry  $\mathcal{M}_{3,5} = \lambda_1, \lambda_7$  then the “shortest” way to

navigate from sheet 3 into sheet 5 is to first encircle branch point  $\lambda_1$  and then branch point  $\lambda_7$ . The path is shortest in a graph-theoretic sense: it includes the fewest possible discriminant points as found by a depth-first search. As branch points are discriminant points, the list  $\mathcal{M}_{1,k}$  defines a path

$$\Pi_{1,k} = \Pi_j, \Pi_{j'}, \dots$$

where the paths  $\Pi_j, \Pi_{j'}$  were computed in Section 3.1.

### 3.2 Lifting paths to the Riemann surface

Computing  $\mathbf{A}(P^\ell, P)$  requires the computation of integrals of the form  $\int_\gamma \omega$ , where  $\omega$  is a normalized holomorphic differential, and  $\gamma$  is a parameterized path on  $\Gamma$  such that

$$\gamma(0) = P^\ell, \quad \text{and} \quad \gamma(1) = P.$$

A parameterized path  $\gamma \in \Gamma$  is uniquely determined by a parameterized path  $\chi \in \mathbb{P}^1$  and an initial value  $y = \mu$  that solves  $F(\alpha^\ell, \mu) = 0$ . We assume the path  $\chi$  from  $\alpha^\ell$  to  $\alpha$  avoids all discriminant points unless  $x = \alpha$  is itself a discriminant point. The path  $\chi$  has  $n$  distinct images on  $\Gamma$ , each of which may be uniquely determined by analytically continuing one of the elements of  $\mathbf{y}^\ell$  along  $\chi$ . The path  $\gamma$  is the image of  $\chi \in \Gamma$  for which the starting place  $\gamma(0) = (\alpha^\ell, \mu)$ . For the purposes of integrating holomorphic differentials this determination is unique up to elements of  $\mathcal{H}$ .

Our algorithms perform analytic continuation along a path  $\chi$  using two methods, namely numerical analytic continuation and Puiseux expansions.

- **Numerical analytic continuation:** If a path  $\chi \in \mathbb{C}$  begins and ends respectively at regular points  $x = \alpha_0$  and  $x = \alpha_1$ , then the values of  $\mathbf{y}(\alpha_0)$  follow paths on the Riemann surface from simple roots of  $F(\alpha_0, y) = 0$  to simple roots of  $F(\alpha_1, y) = 0$ . If  $\alpha_1$  is close to  $\alpha_0$ , and  $\chi$  is nearly a straight line path avoiding discriminant points, then  $\mathbf{y}(\alpha_1)$  is well approximated by

$$\mathbf{y}(\alpha_1) = \mathbf{y}(\alpha_0) + \mathbf{y}_x(\alpha_0)(\alpha_1 - \alpha_0) + \mathcal{O}(|\alpha_1 - \alpha_0|^2),$$

and the last term is small in comparison with the first two. Here  $\mathbf{y}_x$  is the  $n$ -tuple of derivatives of the algebraic function  $\mathbf{y}$  at the point  $\alpha_0$ . By implicit differentiation

$$\mathbf{y}_x(\alpha_0) = - \left( \frac{F_x(\alpha_0, y_1(\alpha_0))}{F_y(\alpha_0, y_1(\alpha_0))}, \dots, \frac{F_x(\alpha_0, y_n(\alpha_0))}{F_y(\alpha_0, y_n(\alpha_0))} \right),$$

where the subscripts  $x, y$  denote partial differentiation. Comparing the unordered  $\mathbf{y}(\alpha_1)$  with the ordered approximation given by  $\mathbf{y}(\alpha_0) + \mathbf{y}_x(\alpha_0)(\alpha_1 - \alpha_0)$  results in an ordered  $n$ -tuple  $\mathbf{y}(\alpha_1)$ . This method may not resolve the order properly if  $|\alpha_1 - \alpha_0|$  is too large or the path from  $\alpha_0$  to  $\alpha_1$  deviates significantly from a straight line. In this case the path is broken up into sub-intervals and the analytic continuation is performed adaptively, over the smaller segments until the order is correctly assigned. More detail on this is found in [13].

- **Puiseux expansion method:** Analytic continuation near discriminant points is problematic. At a discriminant point  $x = \lambda$  there are less than  $n$   $y$ -values, so the above approach is not possible. Further, in some neighborhood around  $\lambda$ , the  $y$ -sheets are close together, and distinguishing them numerically is difficult. Puiseux expansions resolve these issues.

The path  $\chi$  constructed above from  $\chi(0) = \alpha^\ell$  to  $\chi(1) = \alpha$  avoids almost all discriminant points. The path will avoid all discriminant points if  $\alpha$  is not inside  $C_j$  for some  $j$ . If any part

of  $\chi$  is inside  $C_j$  we use the Puiseux expansions over  $\lambda_j$ , the center of  $C_j$ , to represent the sheets of the Riemann surface within  $C_j$ . The rest of  $\chi$  is lifted to  $\Gamma$  via analytic continuation.

Let  $\tilde{z}$  be the value of the path parameter such that  $\chi(\tilde{z})$  is the point where  $\chi$  and  $C_j$  intersect. By the construction of  $\chi$  there is only one such point. The  $y$ -sheets are ordered over  $\chi(\tilde{z})$  with respect to  $\alpha^\ell$  by numerical analytic continuation. Denote the ordered  $y$ -values by  $\mathbf{y}^\ell(\chi(\tilde{z}))$ . Let  $\hat{P} = (P_1, \dots, P_n)$  be the  $n$  branches over the discriminant point  $\lambda_j$ . The intersection point  $\chi(\tilde{z})$  is closer to  $\lambda_j$  than any other discriminant point, thus Newton's Theorem assures us that the branches representing the  $y$ -values converge over  $\chi(\tilde{z})$ . Therefore the  $n$  branches can be ordered with respect to  $\alpha^\ell$  by matching  $P_j$  to one of the elements of the ordered  $n$ -tuple  $\mathbf{y}^\ell(\chi(\tilde{z}))$ . Suppose that

$$P_j = \begin{cases} x &= \lambda_j + t^{r_j} \\ y &= \beta_j t^{s_j} + \beta'_j t^{s'_j} + \dots \end{cases}, \quad t \in [0, 2\pi/r_j).$$

The  $y$ -value over the point  $\chi(\tilde{z})$  represented by this branch is  $\beta_j \tilde{t}^{s_j} + \beta'_j \tilde{t}^{s'_j} + \dots$ , where

$$\tilde{t} = \sqrt[r_j]{\chi(\tilde{z}) - \lambda_j},$$

and as this is a convergent series it necessarily matches one of the elements of  $\mathbf{y}^\ell(\chi(\tilde{z}))$ . All the branches are assigned to one of the sheets in this way, and these branches define the local structure of all the places on  $\Gamma$  over  $C_j$ . If  $\alpha = \lambda_j$ , that is if the user specifies a place  $P$  over a discriminant point, then we match only this branch to  $\mathbf{y}^\ell(\chi(\tilde{z}))$ .

Note that only a finite number of terms of Puiseux expansion  $y(t)$  are computed. Thus the above matching is generally done by adaptively refining the branches until the assignments is made correctly over both  $\chi(\tilde{z})$  and the end of the path  $\chi(1)$ .

### 3.3 Integration

Once the paths have been lifted to the Riemann surface computing the Abel map is a matter of integrating holomorphic differentials. The integral

$$\int_\gamma \omega_j = \int_\gamma g_j(x, y) dx = \int_\gamma g_j(x(z), y(z)) \frac{dx}{dz} dz$$

is computable piecewise once the path  $\gamma$  is fixed. In practice a bit more is to be said. Specifically it should be noted that the method of integration is a matter of what form of analytic continuation is used over any particular sub-path. A sub-path lifted to the Riemann surface by means of numerical analytic continuation is integrated using internal Maple routines (adaptive numerical integration). Paths lifted by Puiseux expansion method are integrated by computing series approximations of the holomorphic differentials. These convergent series of ever higher order are integrated and evaluated term-by-term symbolically.

## 4 Computation and verification

In this section we provide examples of the algorithm by means of a Maple implementation. This implementation of the Abel map is included in the regular distribution of Maple 11 (release: Summer 2007). Updated versions may be obtained at <http://www.amath.washington.edu/~bernard/papers.html>. The examples also serve to verify that these algorithms and implementations are performing as desired. The Maple implementation is called in Maple with the syntax

```
>AbelMap(F, x, y, P1, P2, t, digits);
```

- **F** is a polynomial in only the variables **x** and **y**. The coefficients of **F** may not be floating point numbers, but may be irrational if entered as radicals or using the Maple `RootOf` notation.
- **P1** and **P2** are places on the Riemann surface obtained from **F**. Places are entered in three ways.
  - **Regular places:** Places over regular points are entered as  $(x = \alpha + t, y = \beta)$  pairs. For example, on the curve arising from  $F = y^4 + x^4 - 1$ , the point  $x = 2$  is regular, so the place(s) over 2 may be entered in Maple notation (see Appendix) as  
`>P1 := [x = 2 + t, y = RootOf(_Z^4 + 15)];`
  - **Discriminant places and  $\infty$ :** Places over discriminant points and infinity must be entered as truncated Puiseux expansions in the variable **t**. Further, the **y**-series must contain enough terms to distinguish the intended place from all other places over the same point. The curve in Example 3 illustrates this point. There are four places on this curve over  $x = 0$ , and for three of these  $y = 0$  also. Further, for two of these places, the behavior of the  $x$ -component is identical, thus the behavior of the  $y$ -component must be entered explicitly to distinguish the places. For instance,  $P_2$  would be entered as  
`>P2 := [x = t, y = 2*t];`  
 It is possible that an arbitrary finite number of terms of the  $y$ -components must be specified to distinguish between places. It is highly recommended that users of the Maple implementation use the command `'algcurves/puiseux'` to compute places over discriminant points and  $\infty$ .
  - **The algorithmically chosen left place:** The flag `'ZERO'` signifies that the algorithmically chosen place  $P^\ell$  is to be used. This option is useful when computing the Abel map of a divisor independent of the place  $P'$ .
- **digits** is an integer declaring the desired number of correct digits. The implementation returns a vector of  $g$  complex numbers. Each component of the numerically computed vector should share **digits** significant figures, in both real and imaginary parts, with the symbolically calculated component.

In the Appendix we explain the Maple syntax needed to understand the examples below.

#### 4.1 Demonstrating convergence

The genus four Hurwitz curve given by  $F = y^4 + x^4 - 1$  is not hyperelliptic, and has branch points  $1, i, -1, -i$ . In Figure 6 we demonstrate that the Maple implementation of the algorithm produces a Cauchy sequence as the required accuracy is increased. This figure is created by first computing a sequence

$$\mathbf{A}^{(2)}(P^\ell, P), \dots, \mathbf{A}^{(20)}(P^\ell, P)$$

where  $P = (i, 0)$  and  $\mathbf{A}^{(j)}(P^\ell, P)$  is the Abel map computed with **digits** =  $j$ , and then plotting the base-ten logarithmic difference of the infinity norm  $\|\mathbf{A}^{(j)} - \mathbf{A}^{(j+1)}\|_\infty$ .

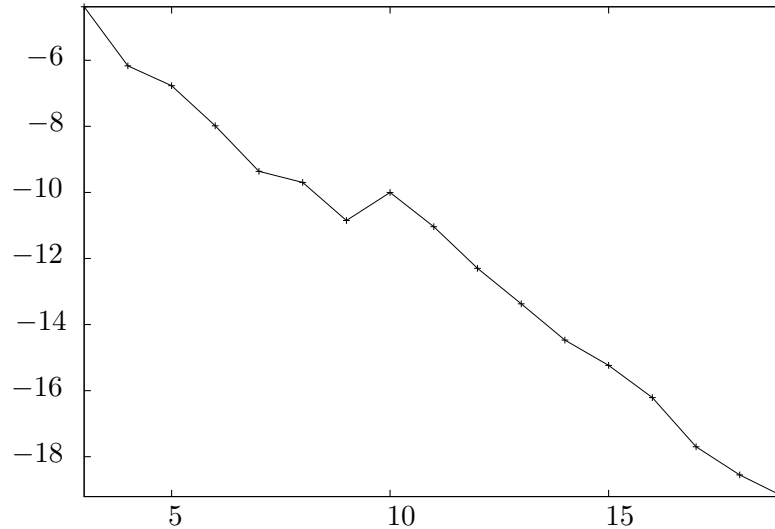


Figure 6: A plot of the convergence of the Maple implementation. The  $j$ -th data point shows the logarithm of the difference between an approximation with  $j$  digits and  $j + 1$  digits of requested accuracy. The “hiccup” in the graph is due to the algorithm obtaining better than expected accuracy for `digits = 9`, and only expected accuracy for `digits ≥ 10`.

## 4.2 A hyperelliptic example

All curves that may be written in Weierstrass form

$$F = y^2 - (x - \lambda_1) \cdots (x - \lambda_{2g+m}), \quad m = 1 \text{ or } 2, \quad \lambda_j \neq \lambda_k, \quad j \neq k$$

are hyperelliptic curves of genus  $g$ . If  $m = 1$  the branch points are the  $2g + 1$  points  $\lambda_j$  and the point at  $\infty$ . If  $m = 2$  the  $2g + 2$  points  $\lambda_j$  are the only branch points.

The Abel map between any two branch points on a hyperelliptic curve is two-torsion [22]. *i.e.*, if  $P', P$  are branch points then, modulo the lattice  $\Lambda$ ,

$$2\mathbf{A}(P', P) = 2 \int_{P'}^P \omega \equiv \mathbf{0}.$$

In what follows the command `ModPeriodlattice(V, B)` returns  $\llbracket \mathbf{V} \rrbracket$ : the vector  $\mathbf{V}$  reduced modulo the period lattice. Thus the unreduced vector is

$$\mathbf{V} = \llbracket \mathbf{V} \rrbracket + \llbracket \mathbf{V} \rrbracket, \quad \llbracket \mathbf{V} \rrbracket \in \Lambda.$$

With the option ‘`fraction`’ the procedure will return the length  $2g$  vector  $\langle \mathbf{V} \rangle$  such that each component  $\langle \mathbf{V} \rangle_j \in [0, 1)$  and  $\llbracket \mathbf{V} \rrbracket = \llbracket \mathbf{B} \rrbracket \langle \mathbf{V} \rangle$ . This option simplifies the detection of vectors that are torsion. We start by reading in the necessary packages and entering a genus 3 plane algebraic curve, and computing its associated Riemann period matrix  $\mathbf{B}$ .

```
>with(algcurves): read("AbelMap.mpl"): # read in the packages
>F:=y^2 - (x^2 - 1)*(x^2 - 4)*(x^2 - 9)*(x - 4); # define a hyperelliptic curve
>B := periodmatrix(F, x, y, 'Riemann'): # calculate the Riemann period matrix
```

$$F := y^2 - (x^2 - 1)(x^2 - 4)(x^2 - 9)(x - 4)$$

Next we compute the places over a sample set of the branch points of our curve.

```

>X := [-3, -2, -1, 1, 2, 3, 4, infinity]; # the branch points of F
># compute the Puiseux expansions over the branch points of F
>puis := 'algcures/puiseux':
>P[1] := op(puis(F, x = X[1], y, 0, t)): P[2] := op(puis(F, x = X[2], y, 0, t)):
>P[3] := op(puis(F, x = X[3], y, 0, t)): P[4] := op(puis(F, x = X[4], y, 0, t)):
>P[5] := op(puis(F, x = X[5], y, 0, t)): P[6] := op(puis(F, x = X[6], y, 0, t)):
>P[7] := op(puis(F, x = X[7], y, 0, t)): P[8] := op(puis(F, x = X[8], y, 0, t)):
>P[6]; P[8]; # display two of the places

```

$$\alpha := [-3, -2, -1, 1, 2, 3, 4, \infty]$$

$$P_6 := [x = 3 - 240t^2, y = -240t]$$

$$P_8 := \left[ x = \frac{1}{t^2}, y = \frac{1}{t^7} \right]$$

Next we define a function `IndexedAbel` such that `IndexedAbel(j, k, digits)` is the Abel map computed from  $P_j$  to  $P_k$  with `digits` significant digits. We compute  $V = \text{IndexedAbel}(6, 8, 10)$ , the Abel map from the place over  $x = 3$  to the place over  $x = \infty$  with 10 significant digits.

```

>IndexedAbel := (j, k, digits) -> AbelMap(F, x, y, P[j], P[k], t, digits):
>V := A(6, 8, 10);

```

$$[.5362947073 - .2163229247 * I, -.5700652852 + .3104163172 * I, .4395355374 - .4252823968 * I]$$

We verify that the vector  $V$  is two-torsion by verifying that  $2\langle V \rangle$  is “nearly integral”. By “nearly integral” we mean  $\|2\langle V \rangle - M\|_\infty$  is small, with  $M \in \mathbb{Z}^{2g}$  the vector closest to  $\langle V \rangle$ .

```

># <V> is denoted by 'BraVKet'
>BraVKet := AbelMap:-ModPeriodLattice(V, B, 'fraction');
># InfNorm computes the infinity norm from the closest integer vector
>InfNorm := z -> max(op(map(w -> abs(round(w) - w), z))):
>DeltaInteger := InfNorm(2*BraVKet); # compute the infinity norm

```

$$\text{BraVKet} := [.3732 \cdot 10^{-13}, .999999999999965, .500000000000197620, .999999999999978,$$

$$.126604458540559303 \cdot 10^{-12}, .5000000000000074]$$

$$\text{DeltaInteger} := .397 \cdot 10^{-12}$$

Figure 7 demonstrates that the Maple implementation of the Abel map is converging. It is constructed as follows. We compute  $8 \times 8$  matrices  $V(\text{digits})$  such that  $V_{j,k}(\text{digits})$  is the Abel map computed from  $P_j$  to  $P_k$  with `digits` significant digits. Each component of  $V(\text{digits})$  is a vector in  $\mathbb{C}^3$ . We reduce each of these vectors modulo the period lattice, and each of these reduced vectors  $\langle V \rangle$  is approximately a half-lattice vector in  $J(\Gamma)$ . We then compute the  $8 \times 8$  matrices `DeltaInteger(digits)` such that

$$\text{DeltaInteger}_{j,k}(\text{digits}) = \|2\langle V_{j,k}(\text{digits}) \rangle - M\|_\infty$$

where  $M \in \mathbb{Z}^6$  is the integer vector closest to  $2\langle V_{j,k}(\text{digits}) \rangle$ . In Figure 7 we graph the base-ten logarithm of the largest component of `DeltaInteger(digits)` for values of `digits` from one to ten.

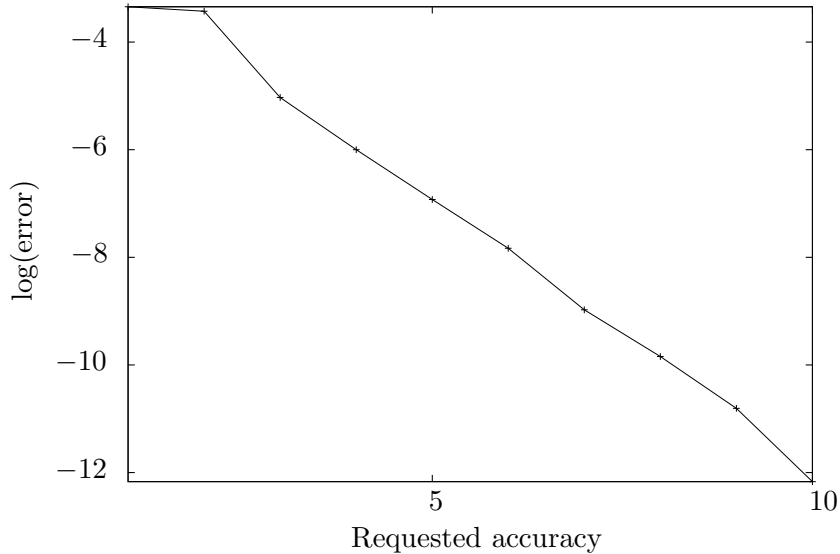


Figure 7: A plot of the convergence of the Maple implementation. The  $y$ -axis is the logarithm of the maximum difference from a lattice vector over all the entries of the matrix  $A$  in Section 4.2. The  $x$ -axis is the accuracy requested.

### 4.3 A non-hyperelliptic example 1

Many algorithms that compute objects associated with Riemann surfaces are restricted in their use. For example it is common for an algorithm to only work in the case of an elliptic, or hyperelliptic curve (please see [19] for definitions of *elliptic* and *hyperelliptic*). To emphasize the general nature of the Abel map algorithm, in the next two examples we work with non-hyperelliptic curves. In this example we use that, by Abel's Theorem, the Abel map of the divisor arising from a meromorphic function is zero modulo the lattice  $\Lambda$ . Specifically we compute the Abel map of the divisor arising from the function  $y$  on the genus 8 surface  $\Gamma$  defined by  $F = y^8 + xy^5 + x^4 - x^6 = 0$ .

```
># define curve F, compute the genus and establish F as non-hyperelliptic
>F := y^8 + x*y^5 + x^4 - x^6; genus(F, x, y); is_hyperelliptic(F, x, y);
```

$$F := y^8 + xy^5 + x^4 - x^6$$

8  
*false*

```
># enter the divisor of the meromorphic function y
>P[1] := [x = -1/t^4, y = -1/t^3 + t^2/8]:
>P[2] := [x = 1/t^4, y = 1/t^3 + t^2/8]:
>P[3] := [x = -1 + t^5/2, y = t]: P[4] := [x = 1 + t^5/2, y = t]:
>P[5] := [x = -t^3, y = t]: P[6] := [x = t^5, y = -t^3]:
>Dvsr := [ [1, P[3]], [1, P[4]], [1, P[5]], [3, P[6]], [-3, P[1]], [-3, P[2]]];
```

$$Dvsr := \left[ \left[ 1, \left[ -1 + \frac{t^5}{2}, y = t \right] \right], \left[ 1, \left[ 1 + \frac{t^5}{2}, y = t \right] \right], \left[ 1, [x = -t^3, y = t] \right], \left[ 3, [x = t^5, y = -t^3] \right], \right. \\ \left. \left[ -3, \left[ x = \frac{-1}{t^4}, y = \frac{-1}{t^3} + \frac{t^2}{8} \right] \right], \left[ -3, \left[ x = \frac{1}{t^4}, y = \frac{1}{t^3} + \frac{t^2}{8} \right] \right] \right]$$

```

># compute the Abel map of Dvsr asking for 10 digits of accuracy
>A := AbelMap:-DivisorAbelMap(F, x, y, t, 'ZERO', Dvsr, 10);

A := [-1.701888413 - 1.660865446 I, - .4032208712 + .2717377626 I, 1.645822432 - 1.590163370 I,
      .911038371 + .8278818528 I, - .2497480507 + 1.152988939 I, .2595511419 - 1.437472396 I,
      -1.222656877 + .8174634287 I, .3898925624 + .4483560160 I]

># compute the Riemann matrix in order to reduce A modulo lattice
>B := algcurves[periodmatrix](F, x, y, 'Riemann'):
># Reduce the vector A
>V := AbelMap:-ModPeriodLattice(A, B);

```

```

V := [.210-9, .9999999948, .104151222 10-8, .999999999, .9999999952, .9999999991, 0.,
      .9999999981, .9999999982, .9999999977, .9999999950, .9999999950, .9999999932,
      .9999999924, .9999999925, .9999999944]

```

The vector V above is approximately the vector  $(0, 1, 1, 1, 1, 1, 1, 0, 1, 1, 1, 1, 1, 1)$ , and thus the vector A is approximately a lattice vector, that is, approximately zero modulo the lattice  $\Lambda$ .

#### 4.4 A non-hyperelliptic example 2

On a genus  $g$  Riemann surface, all divisors  $D_j = (\omega_j)$ ,  $k = 1, \dots, g$  arising from holomorphic differentials  $\omega, \dots, \omega_g$  are linearly equivalent and of degree  $2g + 2$ . For these linearly equivalent divisors we have

$$\mathbf{A}(P, D_1) \equiv \dots \equiv \mathbf{A}(P, D_g).$$

We use this fact to further demonstrate and validate the Maple implementation of the Abel map. Here we change the curve from the previous example slightly to demonstrate the use of algebraic numbers as coefficients.

```

>beta := RootOf(_Z^3 + 7, index = 1): # define an algebraic number
># define a curve and establish that it is not hyperelliptic
>F := y^8 + x*y^5 + x^4 - x^6*beta; is_hyperelliptic(F, x, y);

```

$$F := y^8 + xy^5 + x^4 - x^6\beta$$

*false*

We input the places on the Riemann surface  $\Gamma$  defined by  $F(x, y) = 0$  that constitute the eight divisors  $(\widehat{\omega}_1), \dots, (\widehat{\omega}_8)$  where  $\widehat{\omega}_i$  is the  $i$ -th differential from `algcurves[differentials]`. We choose  $P^\ell$  as the fixed place of the Abel map by using the flag 'ZERO' as an argument of the Abel map. The places we compute next are used to construct the eight canonical divisors.

```

>P[1] := [x = t^5, y = -t^3]; P[2] := [x = -t^3, y = t]; # the two places over x=0

```

$$P_1 := [x = t^5, y = -t^3]$$

$$P_2 := [x = -t^3, y = t]$$

```

># P[3] and P[4] are regular places over the two roots x = sqrt( -beta^2/7 )
>P[3] := [x = 1/2*beta*t^5 + RootOf(beta^2 + 7*_Z^2, index = 1), y = t]:
>P[4] := [x = 1/2*beta*t^5 + RootOf(beta^2 + 7*_Z^2, index = 2), y = t]:
>P[3];P[4];

```

$$P_3 := \left[ x = \frac{1}{2}\beta t^5 + \text{RootOf}(\beta^2 + 7\_Z^2, \text{index} = 1), y = t \right]$$

$$P_4 := \left[ x = \frac{1}{2}\beta t^5 + \text{RootOf}(\beta^2 + 7\_Z^2, \text{index} = 2), y = t \right]$$

```

># there are two branch places over x=infinity, these are P_5 and P_6
>P[5] := [x = -7/(t^4*RootOf(beta^2 + 7*_Z^2, index = 1)^2*RootOf(-RootOf(beta^2
+ 7*_Z^2, index = 1) + _Z^2, index = 1)), y = -7/(t^3*RootOf(beta^2 + 7*_Z^2,in
dex = 1)^2*RootOf(-RootOf(beta^2 + 7*_Z^2, index = 1) + _Z^2, index = 1))]:
>P[6] := [x = -7/(t^4*RootOf(beta^2 + 7*_Z^2, index = 1)^2*RootOf(-RootOf(beta^2
+ 7*_Z^2, index = 1) + _Z^2, index = 2)), y = -7/(t^3*RootOf(beta^2 + 7*_Z^2, i
ndex = 1)^2*RootOf(-RootOf(beta^2 + 7*_Z^2, index = 1) + _Z^2, index = 2))]:
>P[5];P[6];

```

$$P_5 := \left[ x = \frac{-7}{t^4\beta^2\text{RootOf}(-\beta + \_Z^2, \text{index} = 1)}, y = \frac{-7}{t^3\beta^2\text{RootOf}(-\beta + \_Z^2, \text{index} = 1)} \right]$$

$$P_6 := \left[ x = \frac{-7}{t^4\beta^2\text{RootOf}(-\beta + \_Z^2, \text{index} = 2)}, y = \frac{-7}{t^3\beta^2\text{RootOf}(-\beta + \_Z^2, \text{index} = 2)} \right]$$

We form divisors (CD) using integer combinations of these points, compute the Abel maps (A) of these divisors and reduce the resulting vectors modulo the lattice to obtain vectors (V) on  $J(\Gamma)$ .

```

>CD[1] := [[2, P[1]], [5, P[3]], [5, P[4]], [1, P[6]], [1, P[7]]]:
>CD[2] := [[4, P[1]], [2, P[2]], [4, P[3]], [4, P[4]]]:
>CD[3] := [[1, P[1]], [1, P[2]], [3, P[3]], [3, P[4]], [3, P[6]], [3, P[7]]]:
>CD[4] := [[3, P[1]], [3, P[2]], [2, P[3]], [2, P[4]], [2, P[6]], [2, P[7]]]:
>CD[5] := [[5, P[1]], [5, P[2]], [1, P[3]], [1, P[4]], [1, P[6]], [1, P[7]]]:
>CD[6] := [[7, P[1]], [7, P[2]]]:
>CD[7] := [[2, P[2]], [1, P[3]], [1, P[4]], [5, P[6]], [5, P[7]]]:
>CD[8] := [[2, P[1]], [4, P[2]], [4, P[6]], [4, P[7]]]:
>A := i -> AbelMap:-DivisorAbelMap(F, x, y, 'ZERO', CD[i], 8):
>BraVKet := i -> AbelMap:-ModPeriodLattice(A(i), B, 'fraction'):

```

We again use the function `InfNorm`. We construct the  $g \times g$  matrix `DeltaInteger` where the  $j, k$ -th component is the infinity norm of the difference `BraVKet(j) - BraVKet(k)`. As these two vectors are supposed to be identical on  $J(\Gamma)$ , this difference should be nearly integral, and the components of `DeltaInteger` are small if the Maple implementation is computing correctly.

```

>DeltaInteger := Matrix(8, (j, k)-> InfNorm(BraVKet(j) - BraVKet(k))):

```

$$\text{DeltaInteger} := 10^{-7} * \begin{bmatrix} 0.0 & 2.143 & 1.273 & 1.877 & 3.969 & 6.095 & 2.499 & 2.929 \\ 2.143 & 0.0 & 2.401 & 1.254 & 1.826 & 3.952 & 3.235 & 2.474 \\ 1.273 & 2.401 & 0.0 & 2.135 & 4.227 & 6.353 & 1.226 & 1.854 \\ 1.877 & 1.254 & 2.135 & 0.0 & 2.092 & 4.218 & 2.416 & 1.220 \\ 3.969 & 1.826 & 4.227 & 2.092 & 0.0 & 2.126 & 4.508 & 2.373 \\ 6.095 & 3.952 & 6.353 & 4.218 & 2.126 & 0.0 & 6.634 & 4.499 \\ 2.499 & 3.235 & 1.226 & 2.416 & 4.508 & 6.634 & 0.0 & 2.135 \\ 2.929 & 2.474 & 1.854 & 1.220 & 2.373 & 4.499 & 2.135 & 0.0 \end{bmatrix},$$

which confirms the quality of the algorithm and its implementation.

## 5 Applications

As stated in the introduction, our primary motive for computing the Abel map is as part of a program to compute solutions of integrable systems. In the introduction we cite the KP equation as an example. A  $g$ -phase solution of any integrable system is given by an Abelian function, parameterized by a genus  $g$  Riemann surface  $\Gamma$ . Such solutions are given as ratios of homogeneous polynomials of Riemann theta functions and their derivatives [3]. The Abel map appears in the argument of the theta function in the constant vector  $\Phi$  of initial phases, for the KP equation given by

$$\Phi = \mathbf{A}(P^\infty, \mathcal{D}) - \mathbf{K}(P^\infty),$$

where  $P^\infty$  is an infinite place on  $\Gamma$ ,  $\mathcal{D}$  has degree  $g$  and  $\mathbf{K}(P^\infty)$  is the vector of Riemann constants of place  $P^\infty$ . The vector of Riemann constants is given by

$$\mathbf{K} = (K_1, \dots, K_g) : \quad K_j(P) = \frac{1 + \mathbf{B}_{j,j}}{2} - \sum_{k \neq j}^g \oint_{a_k} \left( \omega_k(Q) \int_P^Q \omega_j \right)$$

and can be computed by use of the Abel map. For any  $P \in \Gamma$  and any  $\mathcal{D} = (u)$ , where  $u$  is a meromorphic function on  $\Gamma$ , we have

$$-\mathbf{A}(P, \mathcal{D}) \equiv 2\mathbf{K}.$$

Details of computing the vector of Riemann constants are forthcoming [11].

### 5.1 Integration of algebraic functions

A second motivation for the numerical computation of the Abel map is that it can be used to compute the *torsion* of a divisor. This, in conjunction with a theorem of Risch, can be used to answer the question of whether certain algebraic functions can be integrated in finite terms. The full details of this concept are beyond the scope of this paper and for details the reader is referred to the literature [8, 23, 24, 17]. However, the mathematics used in this section can be gleaned from [19]. We will give an example in which we demonstrate the existence of an elementary anti-derivative by using the Abel map, and then construct that anti-derivative.

For our purposes a *torsion divisor* with torsion index  $\tau \in \mathbb{N}$  is a divisor  $\mathcal{D}$  with the property

$$\mathbf{A}(P', \tau\mathcal{D}) = \tau\mathbf{A}(P', \mathcal{D}) \equiv 0, \quad (19)$$

where  $\tau$  is the smallest positive integer for which (19) holds [8]. The first equality is an identity by the definition of the Abel map applied to a divisor. In order to discuss torsion divisors in relation to the integration of algebraic functions we first define residues, residue divisors and valuations on Riemann surfaces. In these definitions (i)  $\Gamma$  is a Riemann surface, (ii)  $Q$  is a place on that surface, (iii)  $t$  is a local coordinate at  $Q$ , (iv)  $u$  is a meromorphic function on  $\Gamma$  and (v)  $\nu$  is a meromorphic differential on  $\Gamma$ .

- **Valuation:** Near  $Q$  the function  $u$  is given by  $u = t^k h(t)$ , where  $h(0) \neq 0$  and  $k \in \mathbb{Z}$  may be negative or zero and  $h(t)$  is a holomorphic function. The integer  $k$  is the *valuation* of  $u$  at  $Q$ , denoted  $\text{val}_Q(u)$ .

- **Residue:** If the differential  $\nu$  is given near  $Q$  as

$$\nu = \sum_j \nu_j t^j dt,$$

then  $\nu_{-1} = \text{res}_Q(\nu)$  is called the *residue* of  $\nu$  at place  $Q$ .

- **Residue divisor:** The residue divisor  $(\nu)_{\text{res}}$  of a differential  $\nu$  is

$$(\nu)_{\text{res}} = \sum \text{res}_Q(\nu) Q$$

where the sum is over places on  $\Gamma$  for which  $\text{res}_Q(\nu) \neq 0$ . Note that, unlike the divisors of meromorphic functions, the coefficients of  $Q$  in this divisor definition are not to be interpreted as multiplicities.

Given a meromorphic function  $u$  we construct the meromorphic differential  $d \log u = du/u$ . Near  $Q$  we have

$$d \log u = k \frac{dt}{t} + \frac{dh}{h}. \quad (20)$$

As  $h(0) \neq 0$ , (20) shows that

$$\text{res}_Q(d \log u) = k = \text{val}_Q(u),$$

and as  $Q$  is a general place on the surface,  $(d \log u)_{\text{res}} = (u)$ . Note that (20) shows that poles of  $d \log u$  only occur at places  $Q$  where  $\text{val}_Q(u) \neq 0$ , and therefore  $d \log u$  has no poles that do not appear in  $(d \log u)_{\text{res}} = (u)$ . We now make the following proposition, which is essentially one direction of Risch's Theorem [23, 24].

**Proposition 1.** *Suppose  $\nu$  is an Abelian differential of the third kind. Further suppose that*

$$(\nu)_{\text{res}} = \mathcal{D} = \sum_j (p_j P_j - q_j Q_j),$$

where  $p_j, q_j$  are positive integers. If  $\mathcal{D}$  is a torsion divisor, then there exists a function  $u$  such that  $(u) = \mathcal{D}$  and further,  $\nu - d \log u$  is holomorphic.

Since  $\mathcal{D}$  is a torsion divisor there exists a positive integer  $\tau$  such that

$$\tau \mathbf{A}(\mathcal{D}) = \mathbf{A}(\tau \mathcal{D}) \equiv 0.$$

As the sum of the residues of a meromorphic differential is zero [19],  $\deg \mathcal{D} = 0$ . The degree of  $\tau \mathcal{D}$  is also zero, so by Abel's Theorem there exists a function  $u$  such that  $(u) = \mathcal{D}$ .

We showed above that  $(u) = (d \log u)_{\text{res}}$  and that the poles in the residue divisor are the only poles of  $d \log u$ . As  $\nu$  was supposed to be an Abelian differential of the third kind the pole structure of  $\nu$  and  $d \log u$  are identical. Thus the difference  $\nu - d \log u$  is a holomorphic differential. Further, if  $\nu - d \log u = 0$  then  $\int \nu = \log u + c$ .

We use this proposition to integrate an algebraic function. In this example we use the Maple implementation of the Abel map to verify that the residue divisor of (21) is a torsion divisor. Other algorithms and implementations exist for establishing that a divisor is torsion [8, 9]. For instance, using such algorithms the computer algebra system Axiom is able to compute (4). The curve in this example comes from [15], and the methods used are used in [17]. The values of the coefficients of the numerator of (21) are essential for the existence of the anti-derivative.

**Example 4.** *We evaluate the integral*

$$\int \frac{39x^2 + 9x - 1}{\sqrt{x^6 + 4x^4 + 10x^3 + 4x^2 - 4x + 1}} dx. \quad (21)$$

Equation (21) can be seen as the integral of the meromorphic differential  $\nu = (39x^2 + 9x - 1)/y dx$  on the Riemann surface  $\Gamma$  arising from the polynomial

$$F = y^2 - (x^6 + 4x^4 + 10x^3 + 4x^2 - 4x + 1) = 0. \quad (22)$$

We calculate the residue divisor of this differential, and verify that  $\nu$  is an Abelian differential of the third kind. If the residue divisor is torsion we can find a function  $u$  such that  $d \log u = \nu$ . A basis of the holomorphic differentials on  $\Gamma$  is given by  $(dx/y, x dx/y)$ , thus to calculate the poles of  $\nu$  it suffices to calculate the poles of  $\tilde{\nu} = 39x^2/y$ . These may occur where  $y = 0$  or  $x = \infty$ .

- The points for which  $y = 0$  are the six roots  $\lambda = \{x \in \mathbb{C} : F(x, 0) = 0\}$ , that is, the branch points. Using Puiseux expansions, it is straightforward to show that none of these places are poles of  $\nu$ .
- The places over  $x = \infty$  are, labeled by the sign of the  $y$ -series,  $P_{\pm}^{\infty} = (1/t, \pm 1/t^3 + \dots)$ . Substituting this, and  $dx = -1/t^2 dt$  into  $\tilde{\nu}$  yields  $\tilde{\nu} = \mp (\frac{39}{t} + \dots) dt$ , and thus the residue divisor  $(\nu)_{\text{res}} = (\tilde{\nu})_{\text{res}} = 39 P_{-}^{\infty} - 39 P_{+}^{\infty}$ .

Below we show that

$$P_{-}^{\infty} - P_{+}^{\infty} \quad (23)$$

is a torsion divisor with torsion index 39, thus

$$\mathbf{A}((\nu)_{\text{res}}) \equiv 0, \quad (24)$$

proving there exists a function  $u$  such that  $\nu = d \log u$  up to addition of holomorphic differentials. We assume the function  $u = \kappa_1(x)y + \kappa_2(x)$  where  $\kappa_1(x), \kappa_2(x)$  are polynomials in  $x$  (note that this assumption is valid as  $(1, y)$  is an integral basis for the functions with no poles in the affine part of  $\Gamma$  [26]). In order for  $u$  to have a pole of order 39 at  $P_{-}^{\infty} = (x = 1/t, y = -1/t^3)$  and a zero of order

39 at  $P_+^\infty = (x = 1/t, y = 1/t^3)$  we assume  $\deg(\kappa_1(x), x) = 36$  and  $\deg(\kappa_2(x), x) = 39$ . At  $P_\pm^\infty$  both  $\kappa_1(x)y$  and  $\kappa_2(x)$  are degree 39 polynomials in  $1/t$ . We set the leading coefficients of  $\kappa_1(x), \kappa_2(x)$  to one. Solving for all the others such that at  $P_+^\infty$  all terms with  $t$  degree less than 39 vanish gives the required  $\kappa_1(x)$  and  $\kappa_2(x)$  which are given in the Appendix. Calculating  $d \log u$  and simplifying shows  $d \log u - \nu = 0$ . Thus the anti-derivative of  $\nu$  is given by  $\int \nu = \log(\kappa_1(x)y + \kappa_2(x)) + c$ , where  $y = \sqrt{x^6 + 4x^4 + 10x^3 + 4x^2 - 4x + 1}$ .

Here we use the Maple implementation of the Abel map to compute the torsion of divisors on  $\Gamma$  defined by (22). Specifically we establish that (23) has torsion index 39. The points  $-1, 0, 1$  and  $\infty$  are not discriminant points of  $F = 0$ , thus there are  $n = 2$  places on the Riemann surface over each of these points. From any two places in

$$Q_{1,1}, Q_{1,2}, Q_{2,2}, \dots, Q_{4,1}, Q_{4,2} \quad (25)$$

we form a degree zero divisor by taking one place with multiplicity 1 and one with multiplicity  $-1$ . We see that, for a particular basis of the cycles on  $\Gamma$ , the divisors thus formed will have torsion indices of 3, 13 and 39. The command `AllBranches(F, x, alpha, y, 0, t)` below computes Puiseux expansions over the point  $x = \alpha$  with the syntax needed by `AbelMap`.

```
>F := y^2-(x^6+4*x^4+10*x^3+4*x^2-4*x+1); # a hyperelliptic algebraic curve.
>B := periodmatrix(F, x, y, 'Riemann'): # compute the Riemann matrix
```

$$F := y^2 - x^6 - 4x^4 - 10x^3 - 4x^2 + 4x - 1$$

```
># compute the places used to form divisors
>Q[1] := AllBranches(F, x, -1, y, 0, t): Q[2] := AllBranches(F, x, 0, y, 0, t):
>Q[3] := AllBranches(F, x, 1, y, 0, t):
>Q[4] := AllBranches(F, x, infinity, y, 0, t):
>Q[1];Q[2];Q[3];Q[4];
```

$$\begin{aligned} Q_1 &:= [[x = t - 1, y = 2 - t], [x = t - 1, y = -2 + t]] \\ Q_2 &:= [[x = t, y = 1 - 2t], [x = t, y = -1 + 2t]] \\ Q_3 &:= [[x = t + 1, y = 4 + 7t], [x = t + 1, y = -4 - 7t]] \\ Q_4 &:= [[x = 1/t, y = 1/t^3 +], [x = 1/t, y = -1/t^3 +]] \end{aligned}$$

We define a function `IndexedAbelMap` that computes the Abel map  $\mathbf{A}(P^\ell, \mathbf{CD}_{i,j})$  of the divisor

$$\mathbf{CD}_{i,j} = \begin{cases} Q_{i,1} - Q_{j,1} & \text{if } i \neq j \\ Q_{i,1} - Q_{j,2} & \text{if } i = j, \end{cases}$$

and construct a matrix `AbelMatrix` using the function `IndexedAbelMap`. As  $\mathbf{A}(P', P) = -\mathbf{A}(P, P')$ , the matrix `AbelMatrix` thus constructed represents the Abel map from any place in (25) to any other place in (25). We then construct a function `ReduceModLattice` that reduces vectors modulo the period lattice, and apply this function component-wise to the matrix `AbelMatrix`. As we have previously displayed vectors computed by the Maple implementation of the Abel map, in this example we compute but do not display the vectors and reduced vectors. We instead display the results of computing the torsion of divisors  $\mathbf{CD}_{j,k}$

We ask for extra digits of accuracy when computing `DivisorAbelMap` in order to have enough significant digits to correctly assign the torsion index.

```

># define the function 'IndexedAbelMap'
>IndexedAbelMap:=(i, j) -> DivisorAbelMap(F, x, y, t, 'ZERO', 'if'(i<> j, [[1, Q
  [i][1]], [-1, Q[j][1]]], [[1, Q[i][1]], [-1, Q[j][2]]])), Digits + 3):
># construct matrix 'A' using 'IndexedAbelMap'
>AbelMatrix := Matrix(4, IndexedAbelMap):
># construct a function to reduce each vector in matrix 'AbelMatrix'
>ReduceModLattice := V -> ModPeriodLattice(V, B):
># reduce each vector in 'AbelMatrix' modulo the period lattice
>ReducedAbelMatrix := map(z -> ReduceModLattice(z), AbelMatrix):
  The procedure torsion(V, ε) computes the first integer τ such that |τV - [V]| < ε with [V] ∈ Λ.
  We map torsion component-wise to the matrix of vectors reduced modulo the period lattice.
>epsilon := 10^(-8): map(torsion, ReducedAbelMatrix, epsilon);

```

$$\begin{bmatrix} 39 & 39 & 39 & 13 \\ 39 & 39 & 13 & 3 \\ 39 & 13 & 39 & 39 \\ 13 & 3 & 39 & 39 \end{bmatrix}$$

The (4, 4) element of this matrix is the torsion of  $Q_{4,1} - Q_{4,2} = P_-^\infty - P_+^\infty$ , which is indeed 39.

## 5.2 $\mathbb{Z}$ -linear dependence of divisors

The Abel map may be used in conjunction with the LLL algorithm [21] to determine if, given a list of  $m$  divisors  $\mathcal{D}, \dots, \mathcal{D}_m \in \Gamma$ , there exists a linear combination

$$\tilde{\mathcal{D}} = \sum_j n_j \mathcal{D}_j, \quad n_j \in \mathbb{Z}, \quad j = 1, \dots, m$$

such that  $\tilde{\mathcal{D}}$  is the divisor of a meromorphic function. This problem arises, in for instance [7], when determining if certain algebraic functions are algebraically dependent. In what follows we use the Maple implementation of the Abel map to determine a  $\mathbb{Z}$ -linear relation between two divisors.

```

>F := x^4 + (y^2 - 1)*(y^2 - 4) # define an algebraic curve

```

$$F := x^4 + (y^2 - 1)(y^2 - 4)$$

```

>algsurves[puisseux](F, x = 0, y, 0, t); # compute the places over (x = 0)

```

$$\{[x = t, y = 2], [x = t, y = -2], [x = t, y = 1], [x = t, y = -1]\}$$

```

># construct two divisors of the places over (x = 0)
>Dvsr[1] := [[1, [x = t, y = 1]], [-1, [x = t, y = -1]]]:
>Dvsr[2] := [[1, [x = t, y = 2]], [-1, [x = t, y = -1]]]:
>Dvsr[1]; Dvsr[2];

```

```

Dvsr[1] := [[1, [x = t, y = 1]], [-1, [x = t, y = -1]]]:
Dvsr[2] := [[1, [x = t, y = 2]], [-1, [x = t, y = -1]]]:

># compute the Abel maps of Dvsr[1] and Dvsr[2]
>A[1] := AbelMap:-DivisorAbelMap(F, x, y, t, 'ZERO', Dvsr[1], 10):
>A[2] := AbelMap:-DivisorAbelMap(F, x, y, t, 'ZERO', Dvsr[2], 10):
>A[1]; A[2];

[-.304946701650801 + .195053298320151 * I, .304946701634244 - 1.19505329837223 * I,
-.2500000000003239 + .445053298352439 * I]
[.195053298349199 - .1982887 10-10 * I, .304946701634245 - .500000000031671 * I,
.975266491670425 10-1 + .975266491821570 10-1 * I]

># compute the integer dependency of A[1], A[2] (and thus of Dvsr[1] and Dvsr[2])
>ZDependence([A], B, 10);

[4., -4.]

```

Thus  $4Dvsr_1 - 4Dvsr_2 \in \Lambda$ : it is the divisor of a meromorphic function on  $\Gamma$ . Note that the Maple code of the procedure `ZDependence` is included in the Appendix.

## 6 Conclusion

Independent of the application one has in mind, we have presented an algorithm for the numerical computation of integrals of the form

$$I = \int_{P_1}^{P_2} R(x, y) dx,$$

where  $x$  and  $y$  are related by a polynomial relationship:  $F(x, y) = 0$ . Here,  $R(x, y)$  is a rational function of  $x$  and  $y$ , and  $P_1, P_2$  are on the Riemann surface specified by  $F(x, y) = 0$ . Abstractly, we are integrating meromorphic differentials from one point on a Riemann surface to another.

Although we are mainly interested in computing solutions of integrable systems, it is obvious that computing such integrals is an interesting activity in its own right, independent of its connection with integrable systems. In the rest of this paper, we have restricted our attention to the case of the Abel map, *i.e.*, holomorphic differentials. It should be clear from our methods that this is not an essential restriction, as long as  $P_1$  or  $P_2$  are at worst integrable singularities of the meromorphic differential  $R(x, y) dx$ .

## Acknowledgments

We wish to acknowledge Mark van Hoeij for useful conversations, and for pointing out to us the applications of the Abel map described in Sections 5.1 and 5.2. This work was supported by the National Science Foundation through grants DMS-FRG-0139093 (BD), DMS-VIGRE-9810726, DMS-VIGRE-0354131 (MP), DMS-0604546.

## Appendix

We explain the Maple syntax needed to understand the examples in Sections 4 and 5.

- Maple input punctuated with a semi-colon is displayed. Input ending with a colon is not.
- `>'algcures/puiseux'(F, x = alpha, y, 0, t):` computes the places over  $x = \alpha$  in local coordinate  $t$  [13]. That the fourth argument is zero signifies that the  $y$ -series are computed with exactly enough terms to distinguish the  $n$  branches over  $\alpha$  away from  $t = 0$ .
- `>op([1,2,3]);` returns `1,2,3`, *i.e.* removes the outermost set of braces from a list.
- `>map(myfunc, mymatrix, args):` applies function `myfunc` with arguments `args` to each component of matrix `mymatrix`.
- Maple represents general algebraic numbers by using the procedure `RootOf`. For example, `>c := RootOf(_Z^r - 1);` defines `c` as the  $r$ -th roots of unity. More generally, `>c := RootOf(Poly, index = j);` defines `c` as the  $j$ -th root of the polynomial `Poly`.
- `>mypack:-myfunc(myargs):` calls the function `myfunc` from the package `mypack` with the arguments `myargs`.
- `>myfunc := myvar -> generalfunction(myvar):` defines the function `myfunc` inline.
- `>Matrix(N, (j, k) -> g(j, k)):` forms the  $N \times N$  matrix where the  $j, k$  component is the function  $g$  evaluated with arguments  $j, k$ .

The polynomials  $\kappa_1$  and  $\kappa_2$  from Example 24 are given by

$$\begin{aligned}
 \kappa_1(x) = & x^{36} - 9x^{35} + 78x^{34} - 393x^{33} + 1875x^{32} - 6228x^{31} + 20000x^{30} - 44364x^{29} + 100878x^{28} \\
 & - 123754x^{27} + 205056x^{26} + 93834x^{25} + 93210x^{24} + 1154952x^{23} + 1154628x^{22} + 2305452x^{21} \\
 & + 7667343x^{20} + 7398477x^{19} + 18519986x^{18} + 31511637x^{17} + 38292357x^{16} + 68810088x^{15} \\
 & + 94270020x^{14} + 106641612x^{13} + 154404118x^{12} + 169319118x^{11} + 167242404x^{10} \\
 & + 191230470x^9 + 167241762x^8 + 129775188x^7 + 117823332x^6 + 74411808x^5 + 40244337x^4 \\
 & + 28237903x^3 + 10352370x^2 + 2380755x + 1856467, \\
 \kappa_2(x) = & x^{39} - 9x^{38} + 80x^{37} - 406x^{36} + 1986x^{35} - 6636x^{34} + 21881x^{33} - 48249x^{32} + 113386x^{31} \\
 & - 129138x^{30} + 233880x^{29} + 201028x^{28} + 158320x^{27} + 1761084x^{26} + 2213274x^{25} + 4131222x^{24} \\
 & + 13853079x^{23} + 16147329x^{22} + 37199924x^{21} + 69411762x^{20} + 92551930x^{19} + 166484056x^{18} \\
 & + 250442895x^{17} + 308665185x^{16} + 459151006x^{15} + 563317218x^{14} + 607070900x^{13} \\
 & + 732820904x^{12} + 734205504x^{11} + 637517772x^{10} + 621760542x^9 + 479086914x^8 + 303058869x^7 \\
 & + 231510907x^6 + 123527844x^5 + 39445718x^4 + 27825546x^3 + 7163724x^2 - 1856467x + 1332179.
 \end{aligned}$$

The following procedure is used to compute the  $\mathbb{Z}$ -linear dependency of the Abel maps of divisors in Section 5.2

```

ZDependence := proc(V_list :: list, B, acc)
local g, BigZ, i, j, v, N, Lattice, ReducedLattice;
  # Determine 'g', the genus
  g := LinearAlgebra:-RowDimension(B);
  # Determine the number of vectors
  N := nops(V_list);
  # Convert the elements of the vectors to (large) integers
  BigZ := 10^acc;
  v := map(z -> convert(BigZ*z, rational), V_list);
  # Separate the vectors in V into real/imaginary parts, pad with e_j's
  v := seq( [op(map(Re, v[i])), op(map(Im, v[i]))
    , seq('if'(i = j, 1, 0), j = 1..N)], i = 1..N);
  # Construct the lattice 'Lambda'
  Lattice := < 1.*Matrix(g, g, 'shape' = 'identity') | B>;
  # Separate 'Lambda' into real/imaginary and convert to (large)
  # integers, and pad with 'N' zeros
  Lattice := seq(
    [op(map(z -> convert(BigZ*Re(z), rational), convert(Lattice[1..g, i], list)))
    , op(map( z -> convert(BigZ*Im(z), rational), convert(Lattice[1..g, i], list)))
    , seq(0, j = 1..N)], i = 1..2*g);
  # Apply the LLL algorithm
  ReducedLattice := map(z -> evalf(z), IntegerRelations['LLL']([v, Lattice]));
  # Return the linear dependency of the vectors in 'V_list' that give
  # a lattice vector
  return ReducedLattice[1][2*g+1..-1];
end:

```

## References

- [1] M. J. Ablowitz and P. A. Clarkson. *Solitons, nonlinear evolution equations and inverse scattering*. Cambridge University Press, Cambridge, 1991.
- [2] M. J. Ablowitz and H. Segur. *Solitons and the inverse scattering transform*. Society for Industrial and Applied Mathematics, Philadelphia, PA, 1981.
- [3] E. D. Belokolos, A. I. Bobenko, V. Z. Enol'skii, A. R. Its, and V. B. Matveev. *Algebraic-geometric approach to nonlinear integrable problems*. Springer Series in Nonlinear Dynamics. Springer-Verlag, Berlin, 1994.
- [4] G. A. Bliss. *Algebraic functions*. Dover Publications Inc., New York, NY, 1966.
- [5] A. I. Bobenko. All constant mean curvature tori in  $\mathbf{R}^3$ ,  $S^3$ ,  $H^3$  in terms of theta-functions. *Math. Ann.*, 290:209–245, 1991.
- [6] A. I. Bobenko and L. A. Bordag. Periodic multiphase solutions of the Kadomtsev-Petviashvili equation. *J. Phys. A*, 22:1259–1274, 1989.
- [7] E. Compoint and M. F. Singer. Computing Galois groups of completely reducible differential equations. *J. Symbolic Comput.*, 28:473–494, 1999.
- [8] J. H. Davenport. *On the integration of algebraic functions*, volume 102 of *Lecture Notes in Computer Science*. Springer-Verlag, Berlin, 1981.

- [9] J. H. Davenport and B. M. Trager. On the parallel Risch algorithm. II. *ACM Trans. Math. Software*, 11(4):356–362, 1985.
- [10] B. Deconinck, M. Heil, A. Bobenko, M. van Hoeij, and M. Schmies. Computing Riemann theta functions. *Mathematics of Computation*, 73:1417–1442, 2004.
- [11] B. Deconinck and M. S. Patterson. Computing the vector of Riemann constants. *in preparation*, 2007.
- [12] B. Deconinck and H. Segur. The KP equation with quasiperiodic initial conditions. *Physica D*, 123:123–152, 1998.
- [13] B. Deconinck and M. van Hoeij. Computing Riemann matrices of algebraic curves. *Phys. D*, 152/153:28–46, 2001.
- [14] B. A. Dubrovin. Theta functions and nonlinear equations. *Russian Math. Surveys*, 36(2):11–80, 1981.
- [15] N. D. Elkies. [http://www.math.harvard.edu/~elkies/g2\\_tors.html](http://www.math.harvard.edu/~elkies/g2_tors.html)
- [16] H. M. Farkas and I. Kra. *Riemann surfaces*. Springer-Verlag, New York, NY, second edition, 1992.
- [17] E. V. Flynn. Large rational torsion on abelian varieties. *J. Number Theory*, 36(3):257–265, 1990.
- [18] A. P. Fordy, editor. *Soliton theory: a survey of results*. Nonlinear Science: Theory and Applications. Manchester University Press, Manchester, 1990.
- [19] P. Griffiths. *Introduction to algebraic curves*. American Mathematical Society, Providence, RI., 1989.
- [20] P. Griffiths and J. Harris. *Principles of algebraic geometry*. John Wiley & Sons Inc., New York, NY, 1994.
- [21] A. K. Lenstra, H. W. Lenstra, Jr., and L. Lovász. Factoring polynomials with rational coefficients. *Math. Ann.*, 261:515–534, 1982.
- [22] D. Mumford. *Tata lectures on theta. I*. Progress in Mathematics. Birkhäuser Boston Inc., Boston, MA, 1983.
- [23] R. H. Risch. The problem of integration in finite terms. *Trans. Amer. Math. Soc.*, 139:167–189, 1969.
- [24] R. H. Risch. The solution of the problem of integration in finite terms. *Bull. Amer. Math. Soc.*, 76:605–608, 1970.
- [25] G. Springer. *Introduction to Riemann surfaces*. Addison-Wesley Publishing Company, Inc., Reading, MA., 1957.
- [26] M. van Hoeij. An algorithm for computing an integral basis in an algebraic function field. *J. Symb. Comput.*, 18:353–363, 1994.